Fabrication of Nanostructured Manganese Oxide Electrode with M13 Phage Template

by

Jeyeol Hwangbo

A thesis

presented to the University of Waterloo

in fulfillment of the

thesis requirement for the degree of

Master of Applied Science

in

Chemical Engineering

Waterloo, Ontario, Canada, 2013

AUTHOR'S DECLARATION

I hereby declare that I am the sole author of this thesis. This is a true copy of the thesis, including any required final revisions, as accepted by my examiners.

I understand that my thesis may be made electronically available to the public.

Abstract

Applications of biotechnology in drug delivery and medical instrumentation and energy storage have been gaining popularity. Especially, utilization of biotechnology for energy storage is attracting attention due to its environmentally friendly nature and cost efficiency. In this project, a filamentous bacteriophage, M13, to fabricate metal oxide battery electrodes. M13 phage is 6.5 nm wide and 800 nm long, and can act as a template to produce nano-sized metal oxide particles. A method to prepare manganese oxide electrodes was developed, where the phage is integrated with the oxide into a nanocomposite. The composite material was used to make a high capacity electrode for lithium ion batteries. The M13 templated manganese oxide, Mn_3O_4, could deliver a high initial capacity of 766 mAh/g, and recorded a stabilized discharge capacity of ~800 mAh/g even after 60 cycles.

Acknowledgements

Firstly, I would like to express my gratitude to Dr. Pu Chen, my supervisor, for his guidance and supervision throughout my academic terms. Dr. Pu Chen has shaped my ideas and motivated me to finish my work. Without his help, this work could not be completed. Also, I would like to thank Dr. Denise Goosselink for providing abundant experience and knowledge to my research. Her contribution to my study is truly appreciated. Moreover, I am grateful to the team support and stimulating discussions from the battery subgroup members of professor Pu Chen's lab. The working environment and atmosphere are always encouraging. Finally, but most importantly, I want to thank my family for their endless support throughout my university career.

Table of Contents

List of Figures

List of Equations

Chapter 1
Introduction

1.1 Objective

Nanotechnology provides numerous benefits in medicine, biology, material science, and energy storage[2-5]. It has appeared as a popular area of research[1]. Biotemplating is one of the subdivisions of nanotechnology, that can have many industrial applications such as preparation of electrode materials for lithium-ion batteries[2,6].

M13 phage based metal oxides were introduced into biotechnology in 2006. Since then, they have gained attention from many researchers[2]. The M13 phage is an attractive biotemplating material because it is easy to replicate, easy to genetically engineer, and safe to human bodies[2]. So far, numerous M13 based materials have been discovered and applied in various areas of research. The applications of M13 based materials are expected to extend further to many other research areas in the future. In my research project, M13 phage based manganese oxide were synthesized and tested for lithium ion battery applications.

The main objective of my research was to produce manganese oxide nanowires with a biotemplating technique. In particular, I utilized M13 bacteriophage to synthesize various manganese oxide nanowires.

Making M13 phage manganese oxides nanowires is a very challenging task because it is difficult to preserve the surface morphology of M13 phage and to obtain the pure manganese oxide of interest. I applied two experimental approaches to solve these problems. First, all the chemical reactions were carried out at room temperature in order to maintain the surface

morphology of the phage. Second, because manganese oxide formation is very sensitive to the pH of the solution, pH was carefully controlled to 6.5 during the entire incubation process.

Mn_3O_4 and Mn_2O_3 are well-known negative electrode materials for lithium ion batteries and they offer high discharge capacities. MnO_2 is used in various applications including a catalyst in lithium air batteries and positive electrode for lithium-air batteries. My main task in this project was to find suitable methods to synthesize M13 phage templated manganese oxides (Mn_3O_4, MnO_2, and Mn_2O_3) for lithium ion battery applications. In particular, I studied how to manipulate the experimental conditions to produce a high purity and good quantity of Mn_3O_4, MnO_2, and Mn_2O_3 nanocomposites. The specific research objectives of my thesis are:

(1) To optimize the synthesis of M13 based electrode materials at room temperature;

(2) To examine how variables such as concentration, temperature and pH alter the purity and crystallinity of the products;

(3) To develop new methods of synthesizing the nanocomposites while preserving the surface morphology of the M13 phage template;

(4) To establish easy and cost-effective techniques to synthesize manganese oxide nanowires.

1.2 Overview of M13 phage

M13 phage is a filamentous bacteriophage that uses *Escherichia coli* as a host cell. It is about 800 nm in length and 6.5 nm in diameter [23,24]. M13 phage consists of a single-stranded deoxyribonucleic acid (DNA) core surrounded by five major coating proteins (Figure 1.1)[23]

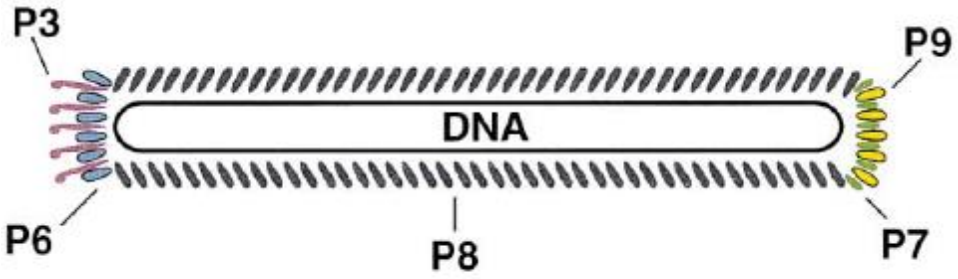

Figure 1.1 Structure of M13 phage [23]

The most abundant among the five coating proteins, pVIII protein plays an important role in producing M13 phage-metal oxide nanowires [24]. In the amino terminus of pVIII, the amino acid residue (AEGDD) is exposed at the phage surface [2.] Amino acids E and G hold negative charge at a neutral pH. Owing to the negative charge on the surface, M13 phage interacts with metal cations via ion exchange[3]. The ion-exchange between the amino acids and metal cations thus plays a vital role in making metal oxide coated nanowires. The overall scheme of the ion-exchange is summarized in figure 1.2.

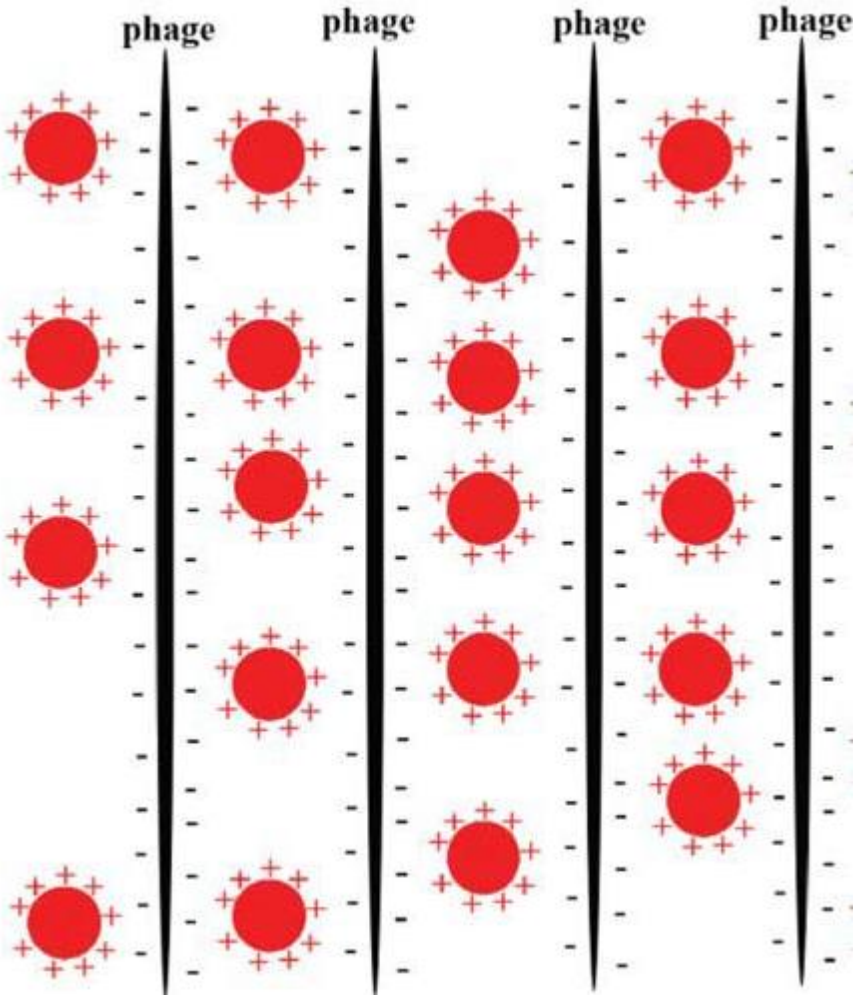

Figure 1.2 Binding of the M13 phage and metal cation in neutral pH [24]

M13 phage-metal oxide nanowires have wide applications in catalysis, MRI imaging, and energy storage [2,3]. In 2006, Belcher's group published an article about a M13 phage biotemplating method for high capacity electrode materials for lithium ion batteries. In this paper, M13 phage was incubated with cobalt (II) solution, and then the cobalt solution was reduced to cobalt (0). Subsequently, the reduction of cobalt was carried out in water[3] to produce Co_3O_4. The production of M13-Co_3O_4 nanowires exhibited nanowire surface

morphology[4] (figure 1.3). The work suggested that once biotemplate is integrated into a battery system, it can significantly improve the battery performance.

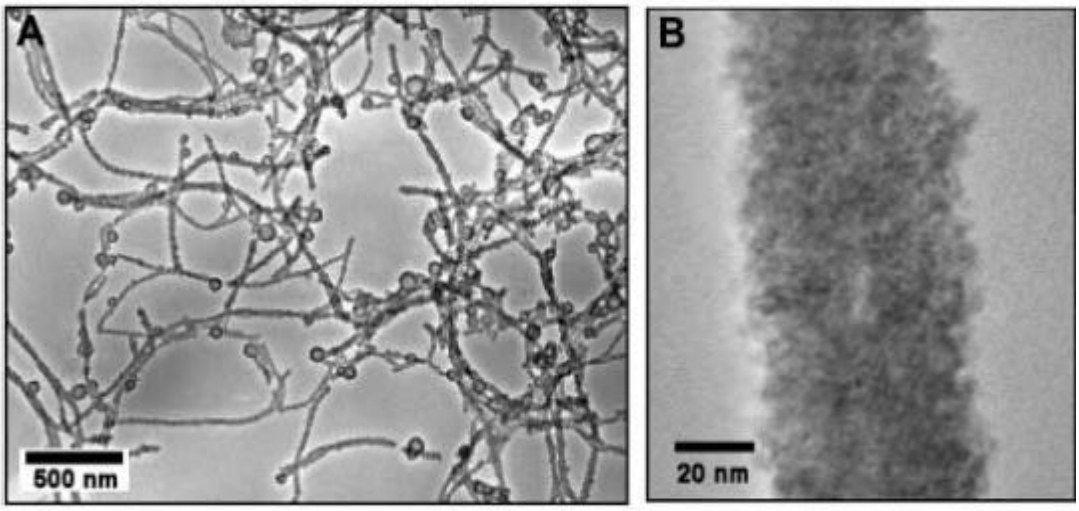

Figure 1.3 TEM image of M13- Co_3O_4 nanowires[23]

1.3 Outline of the thesis

Chapter 1 outlined an overview of the thesis, including the brief introduction of the biotemplating technique, the M13 phage, and my research objectives.

Chapter 2 reviews the literature about applications of the M13 phage template.

Chapter 3 introduces amplification and purification of M13 phage and fundamental principles of the interaction between M13 phage and metal oxides.

Chapter 4 summarizes synthesis of M13-MnO_2 nanocomposite for lithium ion battery applications.

Chapter 5 summarizes synthesis of M13-Mn_2O_3 nanocomposite for lithium ion battery applications.

Chapter 6 summarizes synthesis of M13- Mn_3O_4 nanocomposite for lithium ion battery applications.

Chapter 7 presents the conclusion of the studies and recommendations for future work.

Chapter 2
Literature Review

2.1 Overview

Biotemplating is an ideal tool for synthesizing nanomaterials as it can provide controlled surface morphology, and diversify applications of the products[2,4]. In particular, genetically modified M13 phage is serving as a diverse range of applications such as semi-conductors, micro scale battery, antibacterial sheets, and fluorescence imaging[4,6,7-9]. The application of M13 phage is not only in the lithium-ion batteries, but it also can be used in many medical and electrical applications.

2.2 Relevant applications

Solar Energy Conversion

Sun provides with a staggering amount of energy to the planet ($1.2*10^5$ terawatts), which well exceeds the amount of man generated energy, 13 terawatts[10]. The solar energy is the main source of power that heats the oceans and the planet, and sustains the whole ecosystem[10]. So far, only a small portion of the solar energy is being used to empower human civilization due to low energy conversion efficiency. The major energy sources for mankind are still fossil fuels. However, these fuels are known to cause global warming and environmental damage[10,11]. On the contrary, the solar energy is a clean and renewable energy source and it can be a very attractive solution for solving the energy problems that human civilization is facing[5].

The general mechanism of solar energy conversion is very similar to photosynthesis, which involves the activation of an electron[5]. The general mechanism of solar energy conversion is summarized in figure 2.1[5].

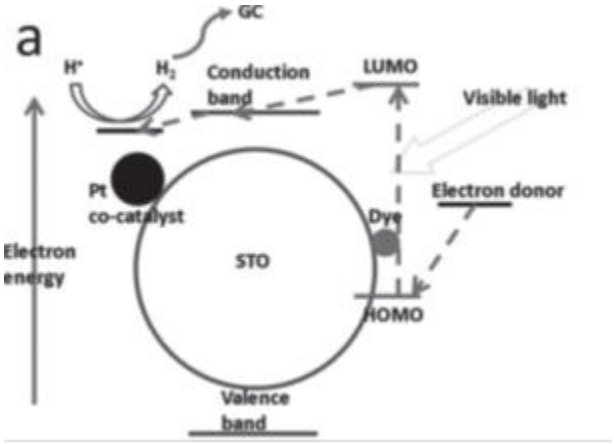

Figure 2.1 Energy band diagram for hydrogen gas production of STO molecules[9]

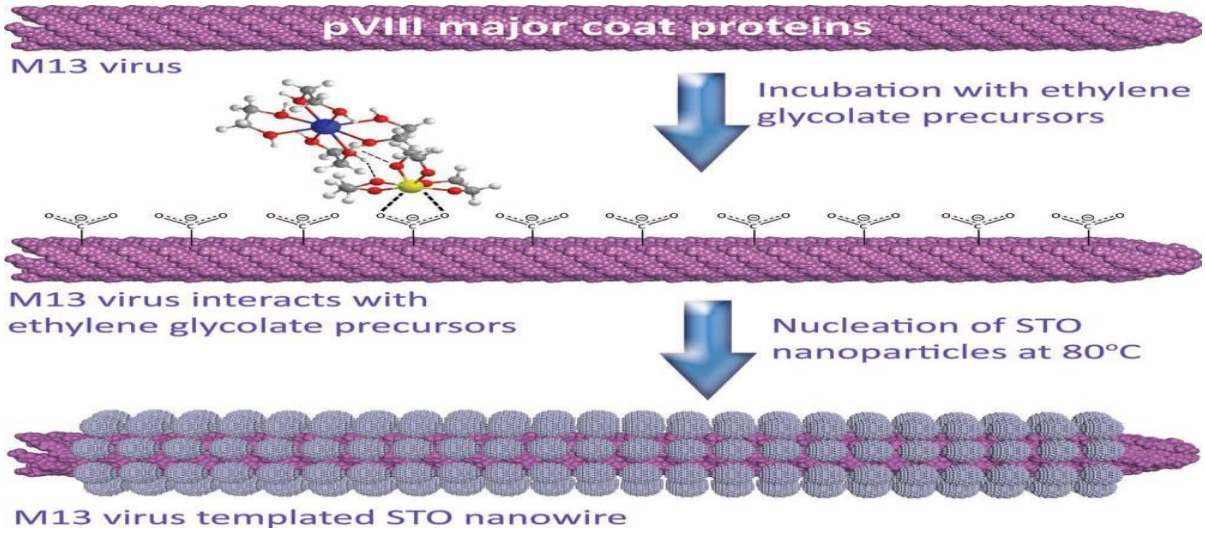

Figure 2.2 Schematics of synthesis of M13 phage templated STO nanowire[5]

Being a common material for solar energy conversion, Strontium Titanate (STO) was mineralized on M13 phage surface. Figure 2.2 summarized the general scheme of STO mineralization on the surface. The virus template material exhibited excellent efficiency in

solar energy conversion. Hydrogen gas production of the material was recorded as 370 μmol/gh, which is ten times higher than that of commercial STO nanopowder and titania[5]. It is thought the superior performance of the material is attributed from the high surface volume ratio and high crystallinity.

Magnetic and Semiconductor Applications

Developing economic and reliable synthesis of one dimensional (1D) material is a fast growing area of research[7]. The use of 1D materials has a very wide range of applications in the field of optical phenomena, functional units in nanocircularity, and electrical transport[12-14]. There are many known approaches of synthesizing magnetic and semiconducting materials such as vapor liquid solid, chemical, solventhermal, vapor phase, and temperature directed fabrication[15-17]. The bio-mineralization of M13 phage was introduced recently for synthesizing 1D material. Due to its high degree of organization and ease of modification of numerous binding motives[2], M13 phage can be a very attractive template material.

The Belcher's group has developed methods to synthesizing 1D material by using genetically modified M13 phage. With phage display technique from the commercial library, the group has screened ZnS, CdS, FePt, and CoPt systems. Productions of metal nanowires include metal salt incubation followed with a reaction between precursor and counterpart ions[7]. The production mechanisms of the metal wires are summarized in figure 2.3.

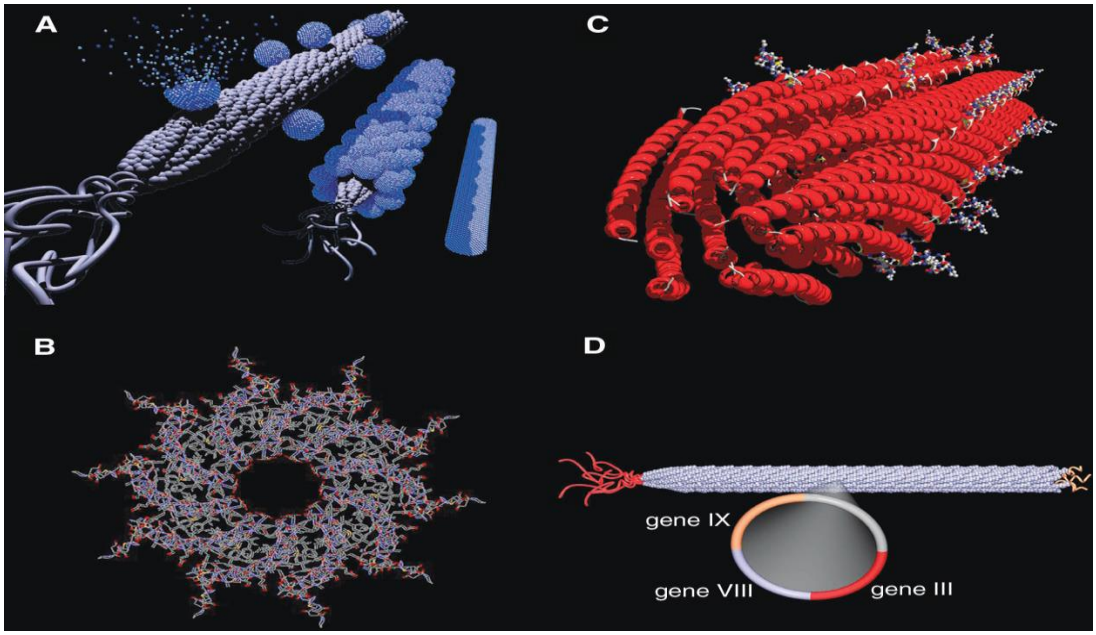

Figure 2.3. summary of nanowire synthesis a) synthesis summary of nucleation, ordering and annealing of nanowire assembly. b) 3D view of nucleated nanoparticles c) summary of nucleation sites in the peptides d) fabrication of nanowire by applying genetic engineering[7].

Based on this summarized reaction schemes, M13 phage templated 1D materials was successfully produced. The synthetic route generated highly ordered nanostructured materials with high crystalinity[7]. Bio-mineralized M13 phage generated 1D nanowires have outstanding properties in many applications such as semiconductor and electric circuits.[7]

Fluorescence imaging of targeted tumor

Among many non-radioactive imaging techniques, fluorescence imaging is one of the most powerful tools for detecting treatment response and disease[6]. Since *in vivo* imaging requires deep penetration depth in tissues, using second near light infrared window light (900-1400nm) could be an ideal tool for *in vivo* application[6]. Therefore, the use of fluorescence imaging, combined with second near light infrared window light, is a very attractive tool for animal testing[6].

Carbon nanotubes are gaining wide attention from the academia due to its high conductivity, good optical properties, and thermal properties[18]. Particularly, with its photoluminescence (PL) properties in the second near light infrared window light (900-1400nm), carbon nanotubes make themselves a very attractive materials for fluorescence imaging[6]. As a matter of fact, the Belcher's group has already introduced functionalized M13 phage and carbon nanotube complex into fluorescence imaging. Figure 2.4 shows the schematic diagram of M13 phage and single walled carbon nanotube complex.

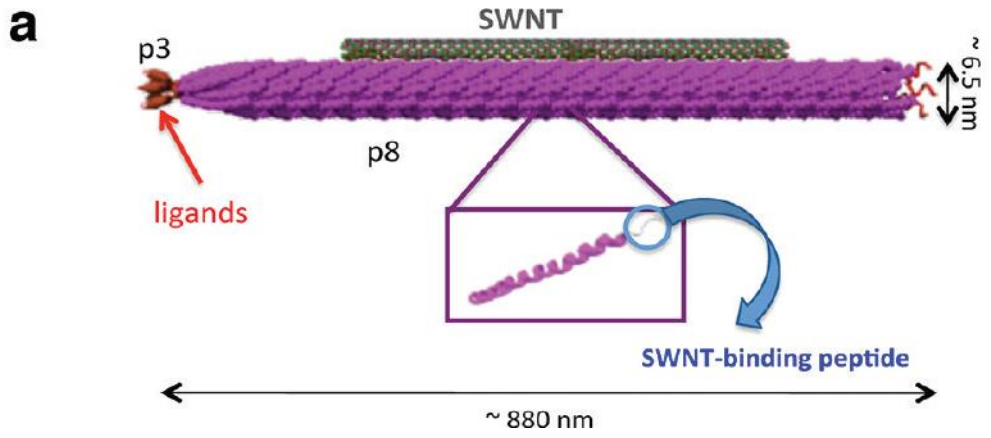

Figure 2.4 M13 phage and single walled carbon nanotube complex[6].

Binding between M13 phage and carbon nanotubes is pH sensitive, and it can be stabilized in aqueous solution for the fluorescence imaging[6]. The pVIII protein, which is the most abundant surface protein of M13, was genetically modified for multivalent binding between M13 and single walled carbon nanotubes[6]. Afterwards, the single walled carbon nanotubes were injected into a tumor bearing mouse for fluorescence imaging and subsequent photoluminescence intensity on the target tumor of a mouse was examined. The M13 and single walled carbon nanotubes complex provided clear images of the target organs, as seen in figure 2.5.

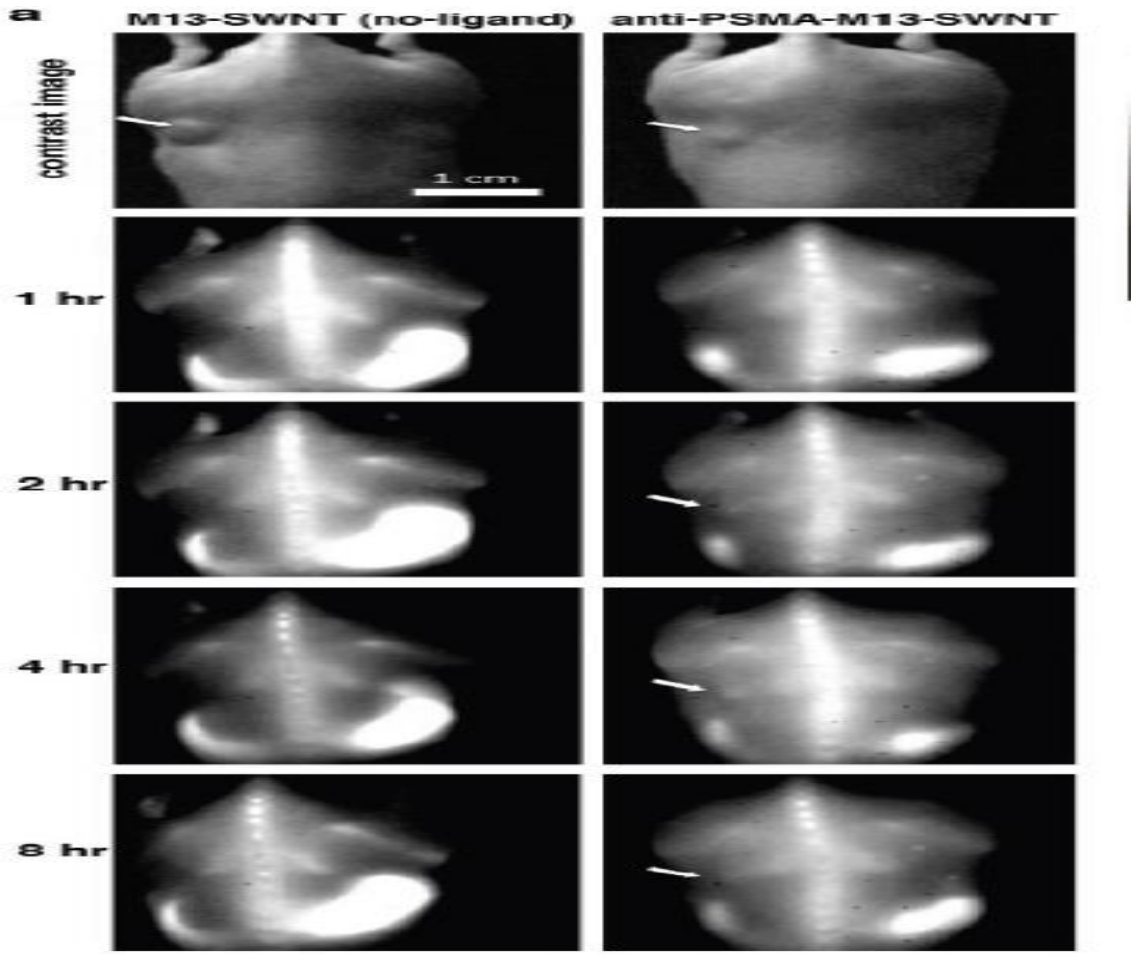

Figure 2.5 *In vivo* imaging of fluorescence imaging of targeted tumor of mouse. Left image is for plasma-M13- single walled carbon nanotubes and the right is for M13-single walled carbon nanotube[6].

In summary, M13 phage successfully served as a template material for single walled carbon nanotubes and binding ligand for fluorescence imaging at second near light infrared window light range[6]. This work was the first attempt to utilize biotemplating materials for *in vivo* image of tumor. Overall, it is one of the successful cases of M13 phage template applications[6].

Phage fiber and coating for antibacterial application

Silver ions and products are known for their antibacterial functions against broad spectrum of microrganisms[9]. Silver compounds promote strong antibacterial action through inhabiting the growth and reproduction of microrganisms[9]. It is thought that silver compounds can interact with bacteria cell membrane and once silver ion is coordinating with bacterial membrane, the cells lose their permeability and eventually lead to death[9.] Despite the strong antibacterial activity, silver compounds are generally safe to mammalian cells. Thus, its value as an antibacterial agent is promising[9].

The Belcher's group has introduced the antibacterial fibers by using M13 template. Before constructing the M13 fibers, the researchers altered the structure of pVIII protein so that the surface contains three glutamic acids instead of one[1-5]. This structure allows a strong binding between silver cations and M13 phage to enhance the performance of M13 phage as a template material for silver compounds[9]. The benefit of M13 phage template is in its surface morphology since the high surface area of M13 increases the interaction between bacterial cells and the silver complexes[9].

In industry, many silver nanostructures are synthesized including nanoparticles and multilayer materials and nanofibers for enhancing antibacterial performance [9, 19-20]. Usually, fabrication of such materials requires template substances such as silica fiber or polymers[9]. Lots of progresses have been made for producing ideal antibacterial materials, but, fabrication of the material is still facing numerous challenges such as limited selectivity and functionality of the template materials[9]. Among the candidate mateials, M13 phage is a good choice as it is free of these limitations. Plus, it offers multiple functionalities and various

ranges of selectivity for metal cations[2,4]. The use of genetic engineering further offers multiple functionalities of the materials and allows significant increase in interaction between metal cations and M13 phage[9].

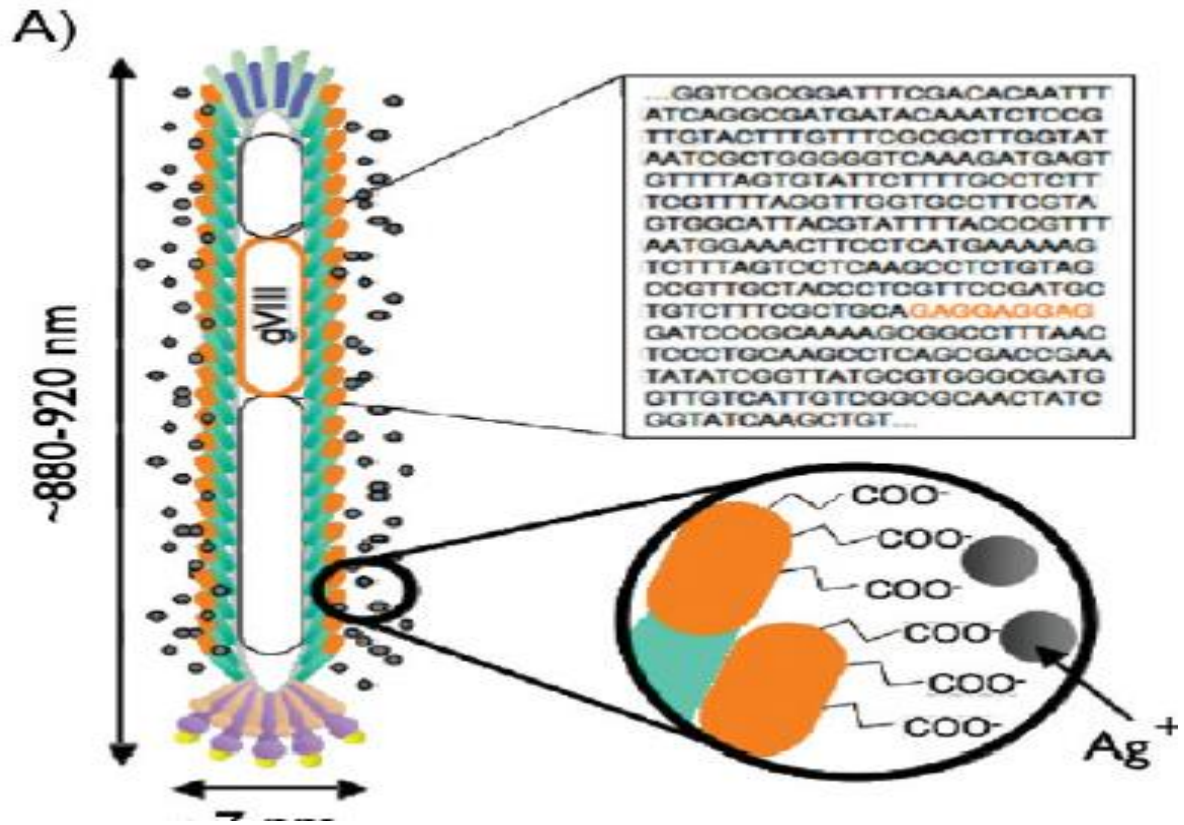

Figure 2.6 Summary of binding interaction between M13 phage and silver cation[9]

Silver nanowires have been produced successfully through binding interaction between the silver ions and M13 phage after addition of sodium borohydride[2,9]. The produced M13-silver nanowires displayed the morphology of M13 phage and they were subjected to test for antibacterial activity afterwards. In the given condition, the genetically modified M13 phage – silver nanowires induced 100% of cell death while non-modified M13 phage- silver

nanowires produced 70% of cell death rate[9].This phage based nanowires can offer a very easy and cost efficient synthetic root for silver nanowires.[9]

Use of phage for energy production

Many research papers have confirmed that M13 based materials can significantly enhance the energy storage efficiency of metal oxides, because the use of template significantly decreases the particle size of the materials[2,3,4]. M13 phage has been used as a template materials for cobalt oxide and iron phosphate, which are very popular electrode materials for lithium ion batteries[2]. The Lee's group has introduced a piezoelectric energy generated from M13 phage thin film because M13 phage has piezoelectric and liquid crystalline properties to generate energy[4].

In order to maximize the energy generation efficiency, this research group applied genetic engineering technique to change the DNA of the phage so that the M13 phage holds 4 glutamic acids on the surface instead of 1 [2,4]. Therefore, the genetically engineered M13 carried 4 times higher charge density than the wild type M13 and this alteration significantly improved the energy generation efficiency[4]. Figure 2.7 and 2.8 summarized the general mechanisms of energy conversion process by using thin layer M13 phage film.

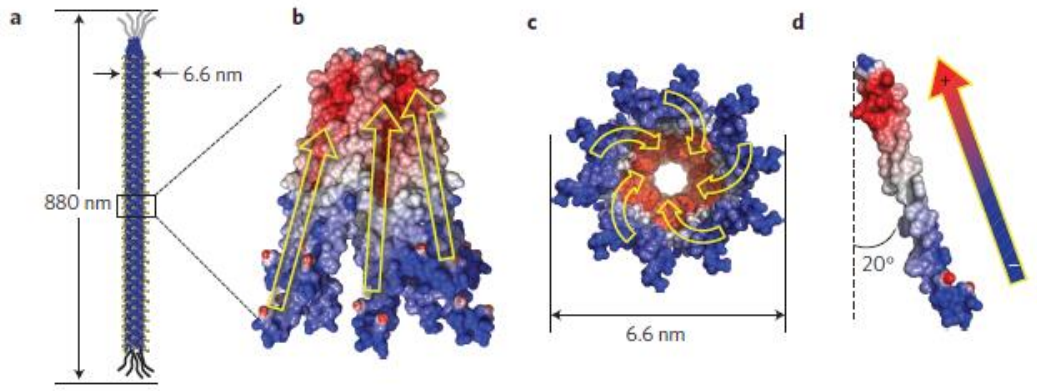

Figure 2.7. a) Shape of M13 phage and its approximate size b) Side view of electric potential generation of M13 phage c) Cross sectional view of electric potential generation of M13 phage d) side view of M13 phage[4]

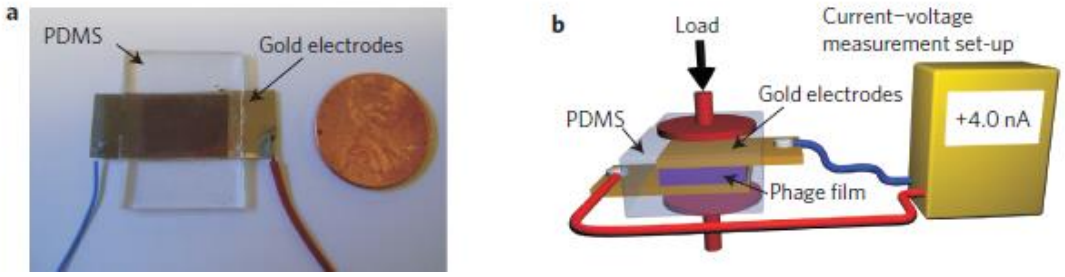

Figure 2.8. a) Picture of the devices b) Schematics of energy measurement from the M13 phage based devices[4].

Overall, the M13 phage film can successfully convert mechanical energy into an electrical energy[4]. The device convert the mechanical energy from the load (figure 2.8 b) and convert into an electrical energy by using dipole moment of M13 phage in the film. This is one of the most important research progresses of M13 phage application so far. It is elucidated that the electrical energy generated from M13 phage film can be correlated with the number of glutamic acids on the surface. For example, the genetically modified M13 (4E) produced about three times more electricity than the wild type phage (1E) under the same

conditions[4]. Relying on the negatively charged amino acids, M13 phage can successfully transfer the mechanical energy into an electrical energy [4].

M13 phage based microelectrode

The advancement of electrical devices has increased the demand for constant and stable supplies of energy[21]. However, the speed of new energy supply development is far behind the advancement of electrical devices[21].Therefore, industry is struggling to provide small scale power sources to satisfy such huge demands [8].

Again, the Belchers group introduced the fabrication of microscale battery electrode materials based on M13 phage[8]. The key challenge of the fabrication of micro battery is to reduce the amount of non-electrochemically active parts[8]. For a typical battery, about 50% of the mass is taken by the non-electrochemically active parts[22]. They have solved this problem by using self-assembly of M13 phage on polymer (LPEI/PAA). The image of M13 phage based electrode was shown in figure 2.9[8].

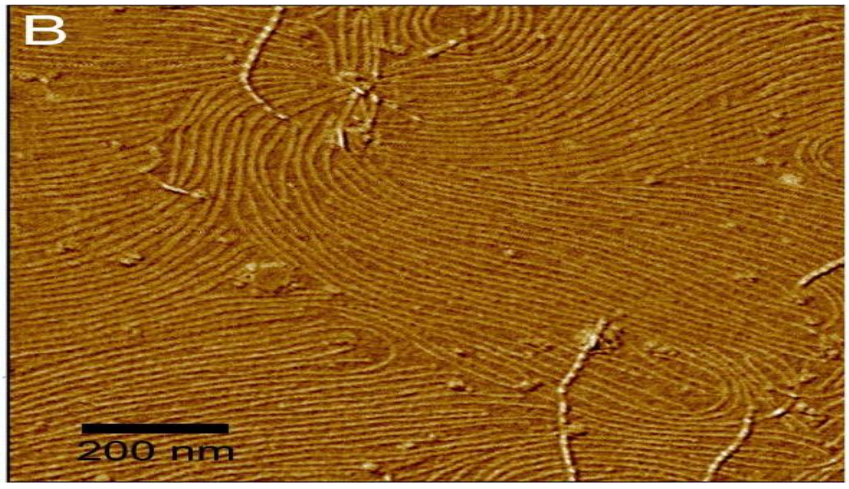

Figure 2.9 AFM image of M13-metal oxide on PDMS[8]

After completion of M13 phage metal oxide complex on polymer, virus based micro batteries were fabricated. The overall schematics of the battery were summarized in figure 2.10.

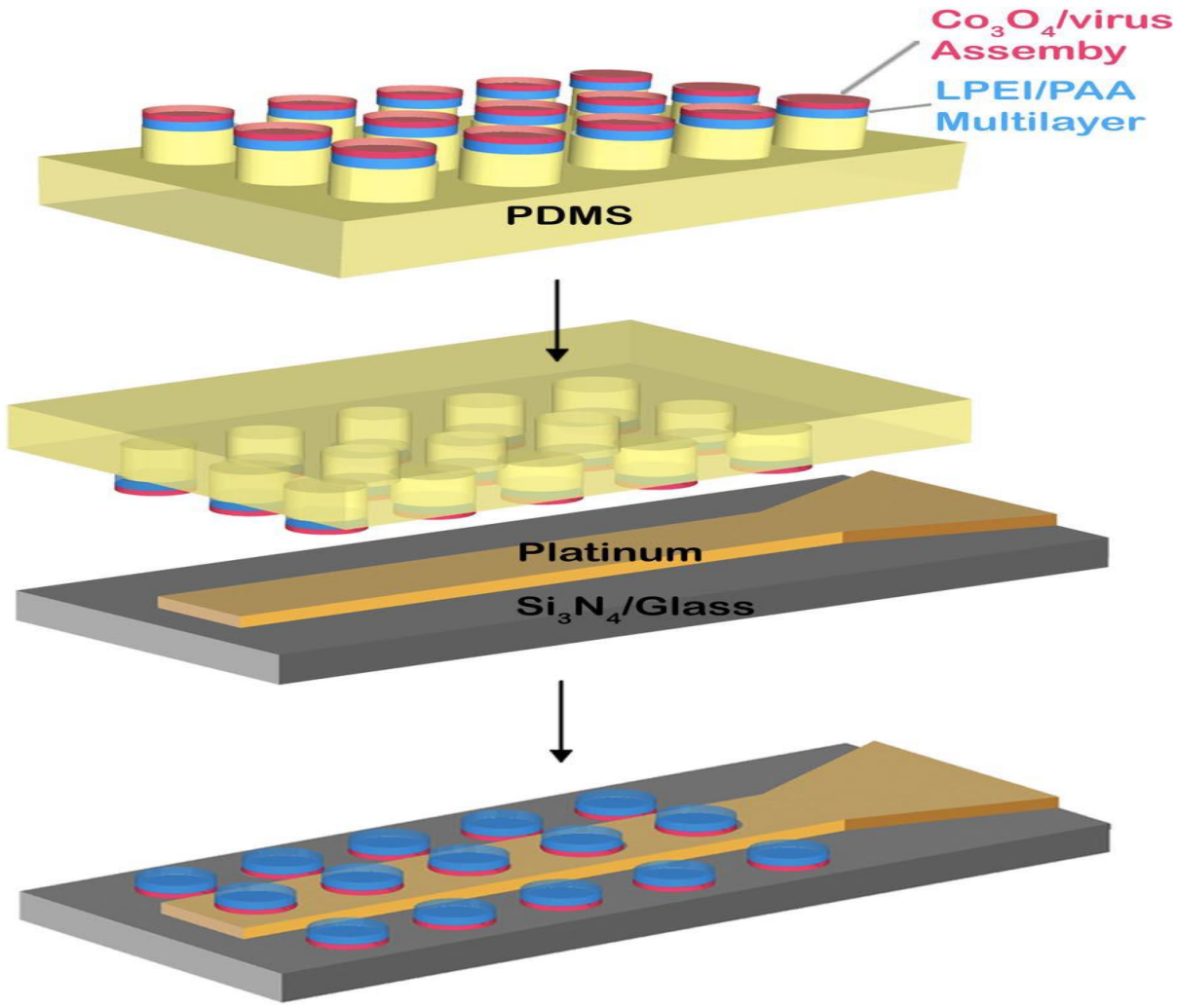

Figure 2.10. Schematics for fabrication of virus based micro battery[8]

The M13 based micro batteries exhibited excellent electrochemical performance and they can be used in varieties of systems[8]. The virus based electrodes can be used for a devices that requires high flexibility[8]. The fabrication of micro battery is the successful case of combination of biology and interfacial phenomena and nanotechnology and polymer

science. Utilization of M13 can be a good boost for fabricating new micro electrode materials and can provide a good and stable energy supplies for micro machines and electronics.

2.3 Conclusion

M13 phage for biotemplating can be used for many applications such as electrodes, energy generation, antibacterial substances, and energy conversion. Many successful research progresses have been reported, and these progresses could be a stepping stone for future research. M13 phage biotemplating techniques are a combination of many academic areas such as computer science, modeling, genetic engineering, interfacial phenomena, nanotechnology, and electronics. Thus, it is a very attractive area of research. As well, it's a prime case of how hybridization of many fields can create a significant outcome.

Chapter 3
Overview of M13 phage and the binding process

3.1 Purification of M13 phage

The polyethylene Glycol (PEG) precipitation method is the most popular technique used for M13 phage purification. However, a recent paper suggested that isoelectric precipitation method could be a better choice for M13 phage purification over PEG method [25]. Figure 3.1 illustrates that isoelectric method had higher purification yield than the one with PEG method. The isoelectric precipitation method purifies the phage solution by changing the pH of the M13 and E coli solution below pH 4.2 [25]. At pH of 4.2, the surface protein of M13 phage loses negative charge and aggregates[25]. The method provides an easy and fast way to produce M13 phage with a high yield. All the detail of the M13 phage amplification and the purification process was referred elsewhere[25].

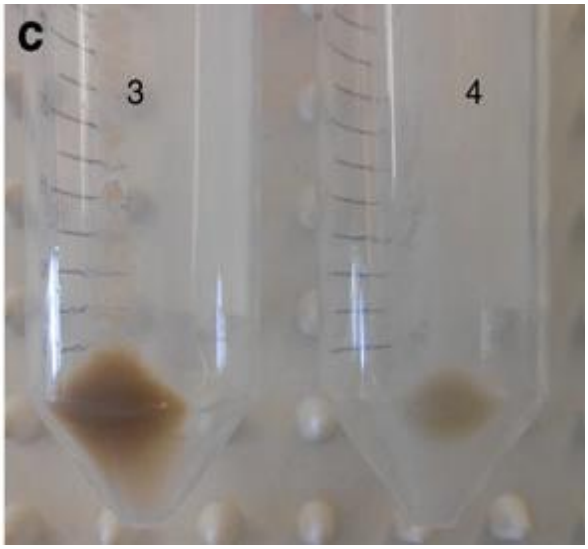

Figure 3.1 Purified phage by using isoelectric (3) and PEG (4) precipitation [25]

3.2 M13 phage metal cation binding process

As mentioned in the previous sections, M13 phage carries negative charges in neutral pH because Glutamic acid (E) and Aspartic acid (D) both have carboxyl groups on their side chains[2]. The negative charge on the surface can have ion-exchange interaction with the metal cation and the interaction force can be defined by Coulomb's law:

$$W(R) = \frac{q_1 q_2}{4\pi\varepsilon_o R} \quad (1)$$

Where

W is a Coulombic interaction energy, ε_o is permittivity of vacuum, q_1 is charge of glutamic acids, q_2 is the charge of metal cations, and R is the distance between metal cation and M13 amino acids.

Also the two charged molecules reveal the electrical force F. This can be summarized as the following equation:

$$F = \frac{q_1 q_2}{4\pi\varepsilon_o R^2} \quad (2)$$

The ion exchange between cations and M13 phage is the key interaction force in this system. Two approaches can be applied in order to increase the binding strength between the cations and M13 phage. The first approach was to increase the surface charge of M13 phage through increasing the number of glutamic acids on the surface proteins. Based on

the M13 phage surface protein structures generated by the Belcher's group through genetic modification, they included 4 glutamic acids on its surface[3]. This alteration maximized the interaction between metal cations and M13 phage and allowed even stronger binding strength between the two. The second approach was to use higher charge density metal cations. Since we are specifically interested in manganese cations, this will not be discussed further.

Chapter 4
Synthesis of M13-Mn_2O_3 nanocomposite

4.1 Overview of Mn_2O_3

Mn_2O_3 is a well-known catalyst for many chemical reactions. For instance, Mn_2O_3 is used for oxidation of ethylene and carbon monoxide[26]. Due to its remarkable catalytic activity in decomposition of environmentally harmful gases, it has gained a lot of attentions from environmental chemists [26]. The production of Mn_2O_3 usually requires high temperature treatment. Generally, Mn_2O_3 is formed by heating MnO_2 to 800 ^oC [26].

A recent article suggested that Mn_2O_3 can be a promising negative electrode material for lithium ion batteries [27]. In this paper, Mn_2O_3 electrode maintained the discharge capacity of 796 mAh/g after 50 cycles. This is a superior electrochemical performance to other common electrode materials such as graphite [27]. Since manganese oxide is a very abundant material in nature, using manganese oxide based electrodes can be a good candidate for electrode materials for lithium ion batteries. Furthermore, manganese oxide material is much cheaper compared with other anode electrode material such as cobalt oxide.

Figure 4.1 Mn_2O_3 crystal

The battery industry is seeking a cost effective way of synthesizing nanocrystalline Mn_2O_3. By using M13 biotemplating, we can successfully produce Mn_2O_3 nanowires. Unlike the other approaches, M13 phage biotemplating simplifies the synthetic procedures. In this chapter introduces the synthesis of Mn_2O_3 nanocomposites by using M13 phage templates.

4.2 . Experimental

4.2.1 Preparation of M13-Mn_2O_3 nanowires

Mn_2O_3 was synthesized with a simple precipitation method followed by heat treatment. Manganese sulfate monohydroxide (1g, Sigma Aldrich) was dissolved in 90mL of distilled water. The solution was stirred at a constant speed for 10 minutes and the resultant solution was mixed with 10mL of M13 phage solution (10^{13} CPU/mL). Thereafter, the phage-manganese sulfate solution was stirred at room temperature for 24 h.

Next, 4.5 mL of 2.5 M sodium hydroxide solution was added to the mixture. After 10 seconds, 20 mL of 2% hydrogen peroxide solution was slowly added into the solution and the mixture formed a black precipitate (figure 4.2). Subsequently, the solution was centrifuged at 5000 rpm for 30 seconds (figure 4.3). The resultant mixture was washed 10 times with distilled water followed by 70% ethanol washing. Then, the precipitate was dried in 100 ^oC oven for 24 hours and was calcined at 700 ^oC for 6 h in air. The resultant compound was grinded by hands and prepared for characterization.

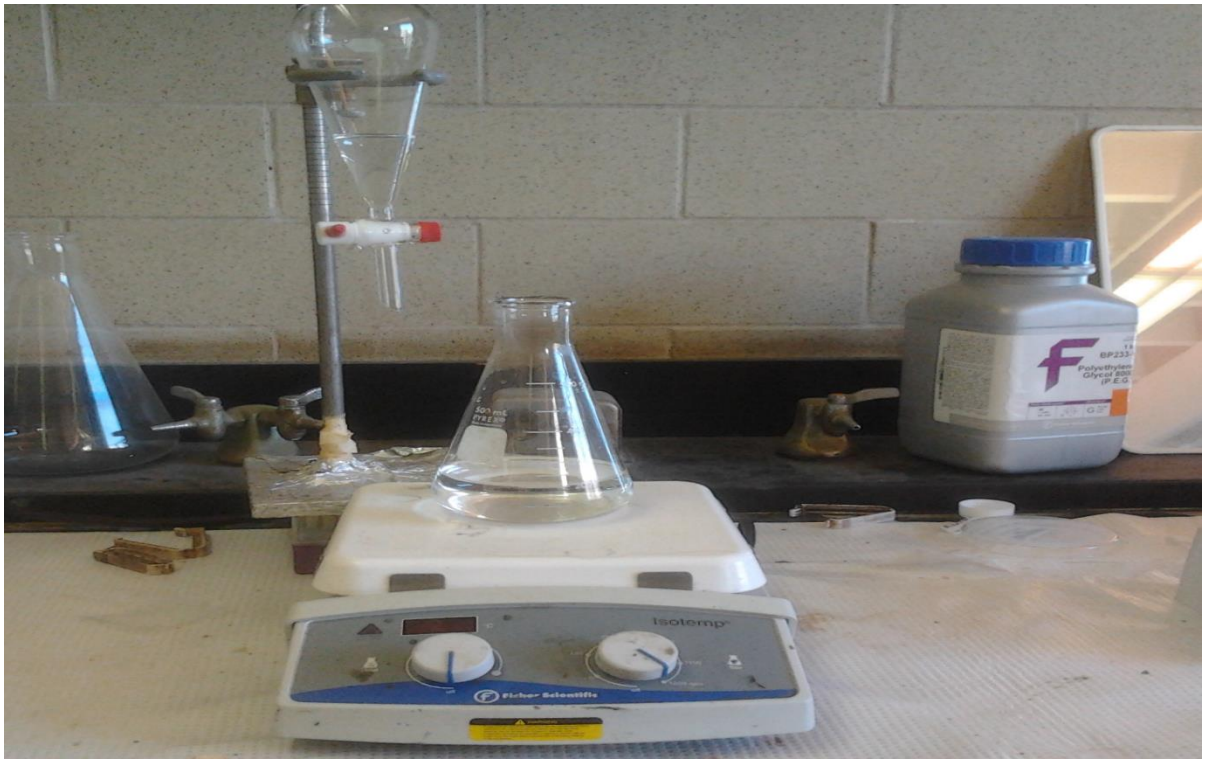

Figure 4.2 General apparatus of the experiment

Figure 4.3 Centrifuge used

4.2.2 Material characterization

The product was analyzed by using X-ray diffraction using Cu kα radiation. The XRD result is summarized in figure 4.5 and 4.6. It is illustrated in the figure that the material was in a good match with Mn_2O_3 indicating a success in producing Mn_2O_3. The surface morphology of the product was also investigated by using Scanning Electron Microscope (SEM, Leo-1530, Zeiss).

4.2.3 Electrochemical measurement

The electrochemical performance of M13- Mn_2O_3 composite samples were tested by using coin type cell (CR2032). Each cell consists of a lithium metal anode and a M_2O_3/acetylene black/polyvynylidene fluoride (PVDF, Kynar, HSV900) cathode. The cathode was made by carefully mixing the 70 wt. % M13-Mn_2O_3 composite, 20 wt. % acetylene black as conductive agent and 10 wt.% PVDF as a binder. The resultant mixture was painted on a copper foil with 1cm diameter and the foil was dried in a vacuum oven overnight at 60^{o}C. The material loaded on the each electrode was about 3mg/cm^2. The cell was tested on galvanostatically on a Neware multichannel battery testers (figure 4.4) between 0.01V-3V *vs* Li^+/Li at current density of 0.1C.

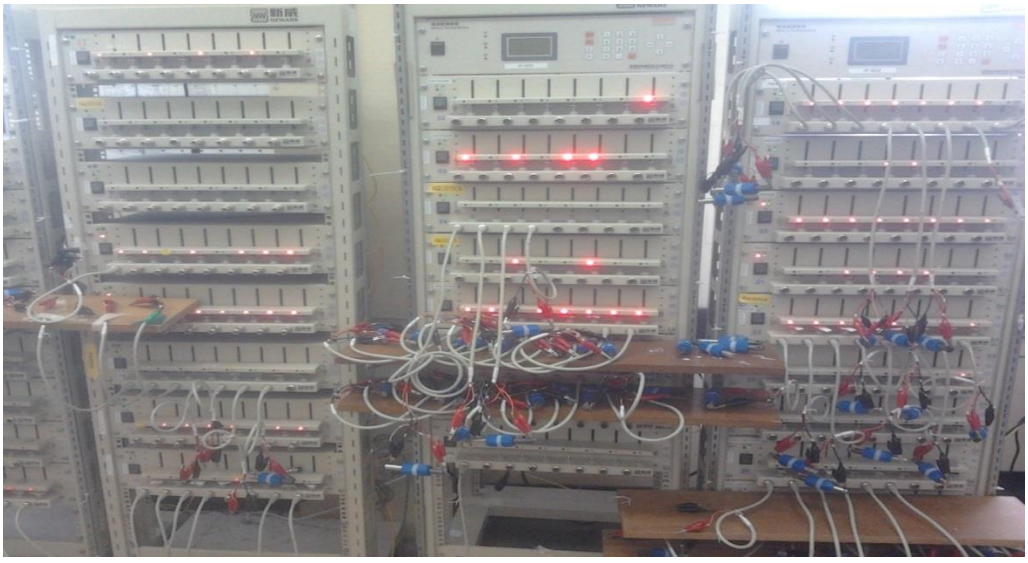

Figure 4.4 Neware multichannel battery tester

4.3 Results and Discussion

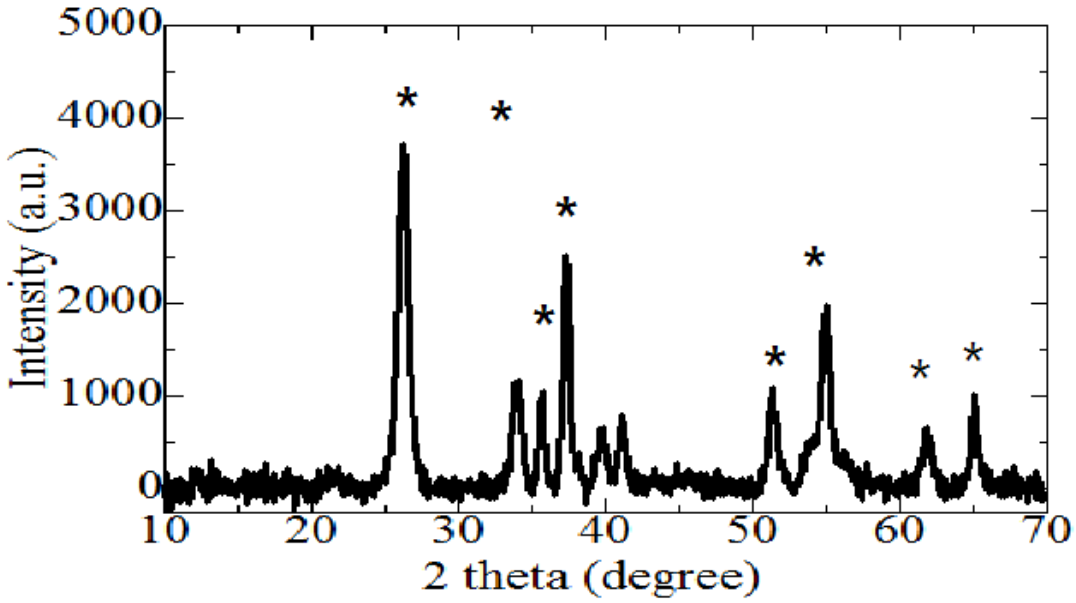

Figure 4.5 XRD pattern of the product before calcination. * represents the reference peaks of MnOOH. Unmarked peaks matches to Mn_2O_3 and MnO_2.

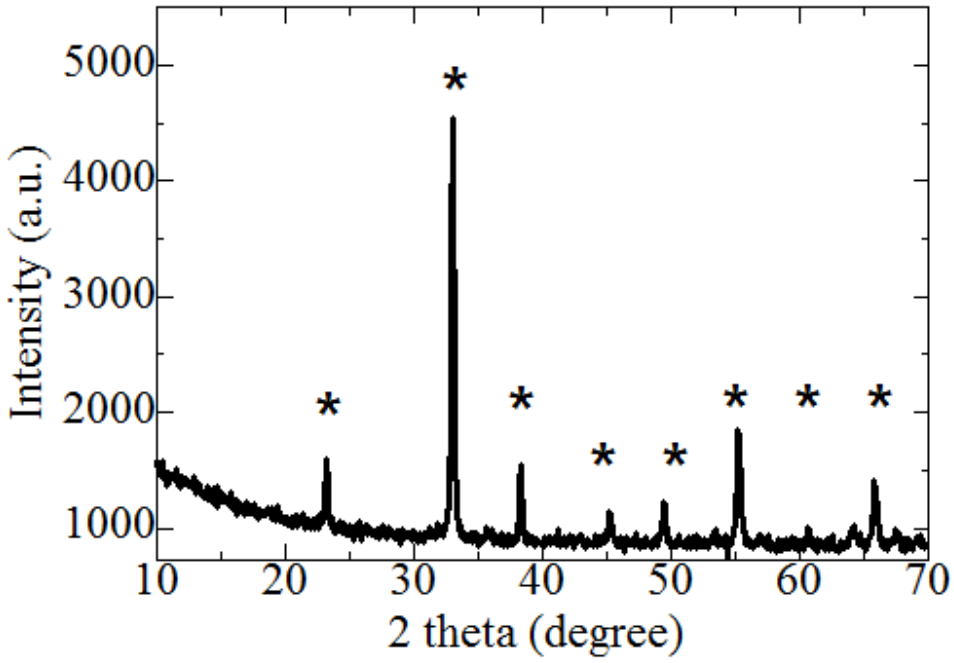

Figure 4.6 XRD pattern of the product nanowire after calcination. * represents the reference peaks of Mn_2O_3.

Addition of hydrogen peroxide produced manganite (MnOOH). However, after the calcination of the product at 700^{o}C, manganite was transformed to Mn_2O_3. The transformation phenomena and the chemistry behind it will be discussed later. When sodium hydroxide is added to the manganese precursor, manganese (II) hydroxide was formed. Addition of low concentration hydrogen peroxide would cause the oxidation of the material to generate MnOOH. The predicted reaction pathway is summarized in figure 4.7.

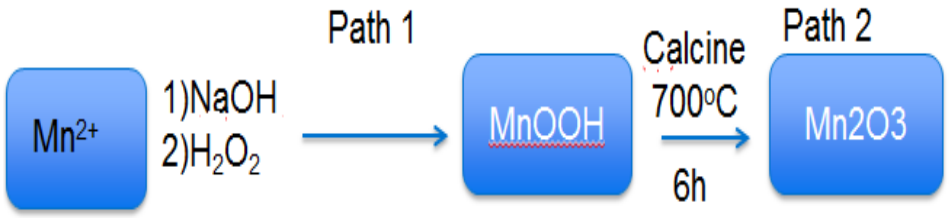

Figure 4.7 Summary of the reaction path

From XRD analysis, the present data confirmed that the reaction path indeed produced Mn_2O_3. Although some impurities such as MnOOH and MnO_2 were detected, most of the product was Mn_2O_3. After checking the purity of the product, the surface morphology of the material was carefully examined. Since the calcination temperature was set to 700^{o}C, it is very likely that the surface morphology of the particles have been altered during the reaction. Besides, hydrogen peroxide is a very volatile substance and can damage the protein structure of M13 phage template.

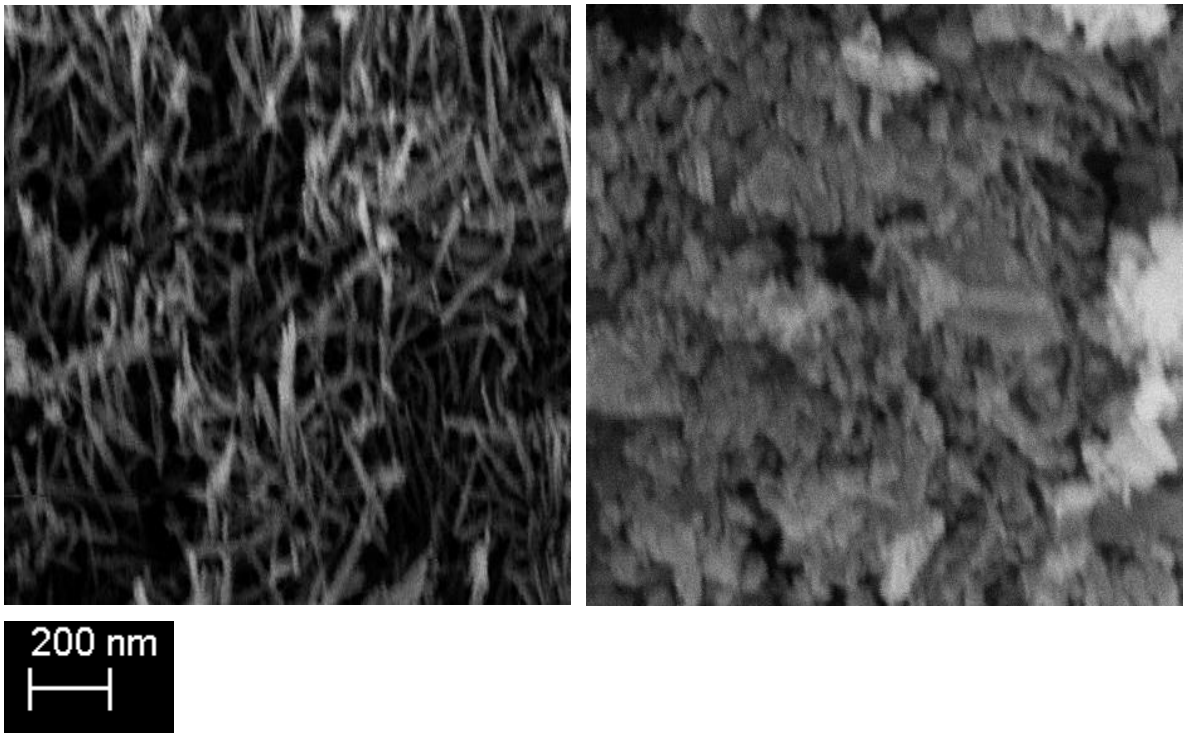

Figure 4.8 Product before calcination with M13(left) and without M13 (right). Both of the products were MnOOH.

As presented in figure 4.8, hydrogen peroxide treatment did not damage the surface morphology of the templating material because we still can observe the fibrous structure. Apparently, the material was about 20 nm in width and 800nm in length that matches to the size of the M13 phage. Nanowires were showed clearly as the morphology as what we aimed for. Base on this observation, the low concentration hydrogen peroxide did not destroy the surface morphology of the material. Possible explanations for the preservation of the surface morphology include: (1) the reaction was instant since black precipitate and bubble (likely oxygen) were formed instantly after addition of hydrogen peroxide and the manganese oxide was formed before the surface morphology of the phage was destroyed; (2) reaction might be hydrogen peroxide concentration dependent. To verify this hypothesis, the phage was

incubated in 0.1% hydrogen peroxide solution for 24 hours and then checked the reproducibility of the M13 phage.

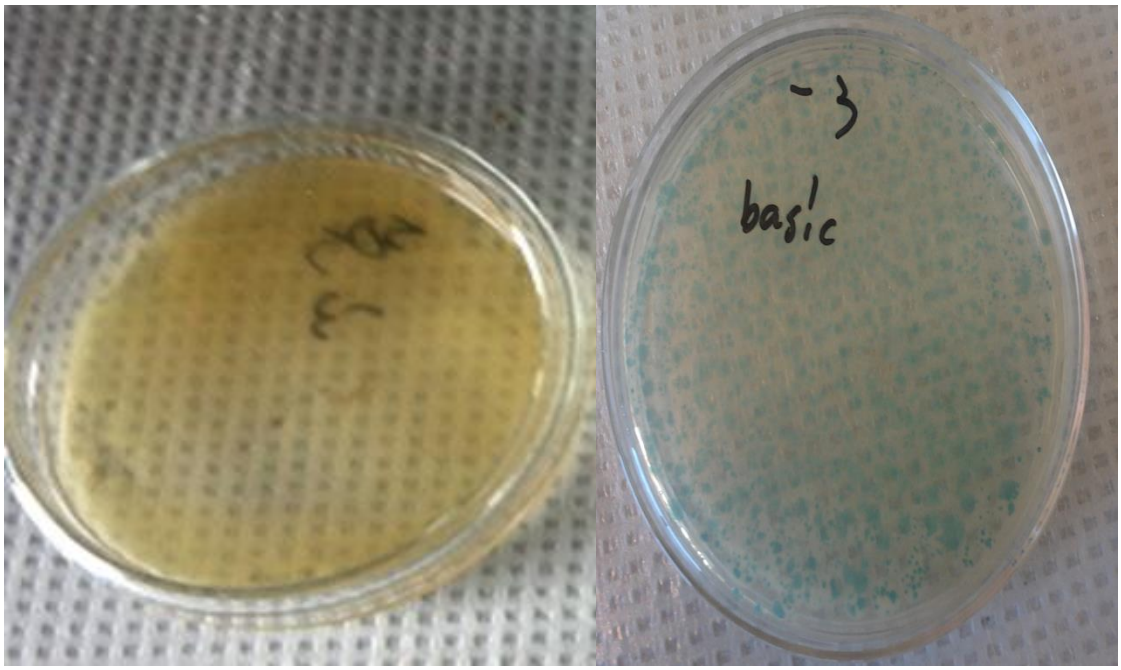

Figure 4. 9 M13 phage incubated in 0.1% H_2O_2 solution (left) and in TBS buffer (right). Green colonies are the M13 phage colonies.

Figure 4.9 reveals that the phage lost its reproducibility after incubation in hydrogen peroxide solution. Even 0.1% solution was enough to suppress the reproducibility of M13 phage. The result manifested that the structure of M13 phage can be changed even in very low H_2O_2 concentration. Thus, it is concluded that the preservation of the morphology only depends on reaction speed.

Once the morphology of MnOOH was confirmed, the product was calcined for 6h at 700 ^oC. Subsequently, the material was characterized using SEM to further examine its structure. The morphology of the material is demonstrated in figure 4.10

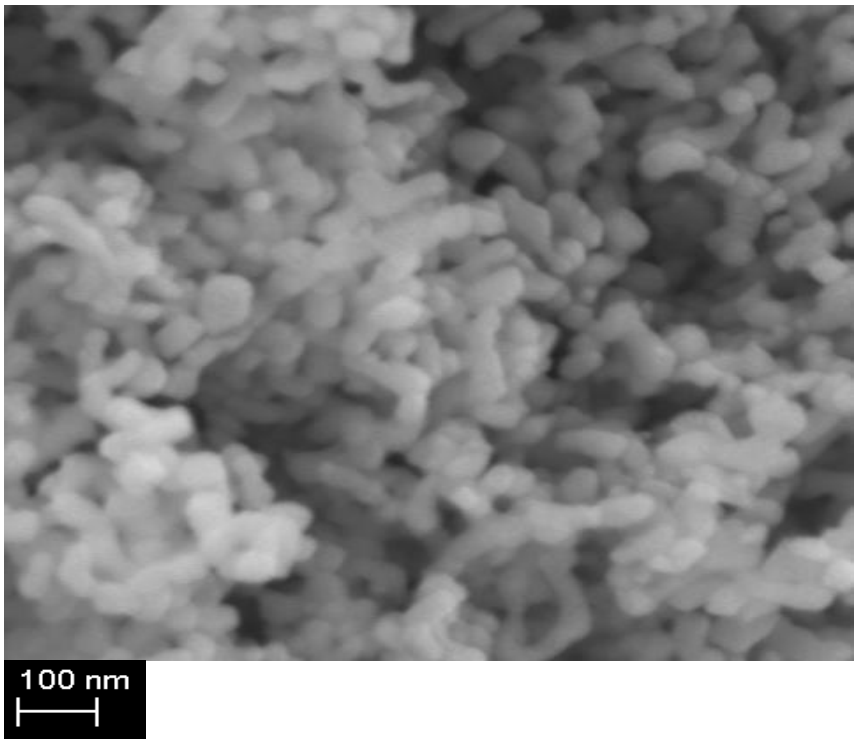

Figure 4.10 Product after calcination

From Figure 4.10, it is revealed that the material was still in nanoscale with a width of 50nm. However, the aggregation of the material was observed which probably due to the high temperature. The main advantage of this fabrication process lies in its simplicity and cost efficiency so it can be produced in a massive quantity of nano Mn_2O_3nanowires.

As mentioned in the introduction, there are many possible applications for Mn_2O_3. However, due to limited resources, only Lithium ion battery application has been investigated thus far. Practically, Mn_2O_3 suffers from its low conductivity[27]. Usually, Mn_2O_3 material is known to have poor capacity retention although straw-sheaf-shaped Mn_2O_3 shows good cycling performance[27]. Due to its high theoretical capacity (1018 mAh/g), Mn_2O_3 can be used as an attractive negative electrode material for lithium ion batteries[27]. Although graphite is the most widely used negative electrode material for Lithium ion battery due to its

good capacity retention and low cost[27], graphite has very low theoretical capacity (372 mAh/g). Accordingly, it is not a very good candidate for high energy density energy storage [27,28]. Equation 3 summarizes the lithium storage mechanism of the material[27].

$$2Li^{+} + 3Mn_2O_3 + 2e^{-} \rightarrow 2Mn_3O_4 + Li_2O \quad (3)$$

$$2Li_{+} + Mn_3O_4 + 2e^{-} \rightarrow 3MnO + Li_2O$$

$$2Li^{+} + MnO + 2e^{-} \rightarrow Mn + Li_2O$$

$$Mn + xLi_2O \leftrightarrow 2xLi^{+} + MnOx + 2xe^{-}$$

Figure 4.11 summarizes the cycling performance of the Mn_2O_3 at current density of 0.1C.

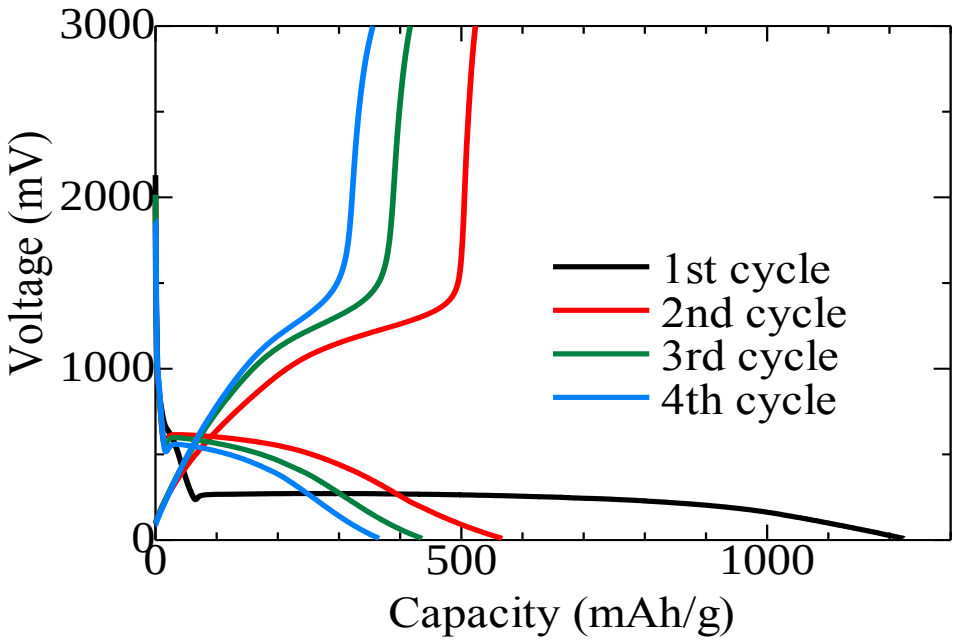

Figure 4.11 Capacity retention of Mn_2O_3 at 0.1C

Although Mn_2O_3 had high initial capacity of 1300mAh/g, the capacity retention of the material was very poor. Just after 6 cycles, the discharge capacity of the material fell below

300mAh/g, which is even lower than the theoretical capacity of graphite. Therefore, we can conclude that the Mn_2O_3 material is not suitable for use as a negative electrode material for lithium ion batteries.

Alternatively, it is possible to use the material for other applications such as catalyst for oxidation of carbon monoxide. The applications of Mn2O3 nanowires need to be investigated further.

4.4 Summary

It is possible to synthesize M13-MnOOH nanowires at room temperature. The calcination of the material at 700 ^oC could cause the transformation of the material e.g. MnOOH was transformed to Mn_2O_3, the end product. Although there was some aggregation of the material, the Mn_2O_3 was still in nanoscale, preserving most of the M13 phage morphology.

The poor capacity retention of the material makes it impossible to be used for Lithium ion battery material. Although the capacity of 796mAh/g was maintained at current density of 0.1C after 50 cycles in some previous research,[27] further investigation is needed to find the suitable applications for the material. Future study on how to use Mn_2O_3 as a catalyst for oxidation of carbon monoxide and ethylene should be perused.

Chapter 5
Synthesis of M13-MnO_2 nanocomposite

5.1 Overview of MnO_2

Since the industrial revolution, the manufacturing sector has been seeking low-cost and reliable energy supplies. This effort has been closely related to technological development and economic growth[29,30]. In the past few centuries, the development of modern civilization has heavily relied on fossil fuels to empower transportation system, machinery and manufactures[29]. However, fossil fuels can only continue empowering humanities for a few more centuries. On the other hand, utilization of fossil fuels produces CO_2 resulting climate change[28]. Many countries are attempting to reduce the fossil fuel usage to protect the planet from the environmental threat. Thus, finding new renewable energy sources is urgently needed for the industries.

Lithium-ion battery is free from greenhouse gas emission and it can be used as energy storage for wind and solar power[29]. However, the technological advancement of Lithium-ion battery is relatively slow compared with other electrical devices such as mobile phones and digital cameras[21]. The energy density and capacity of Lithium-ion battery currently can't satisfy the demands of rising portable electronics industries and information technology[21]. In fact, the advancement of electrical vehicle and cell phone is slowed down due to the poor performance of Lithium-ion battery[21]. Consequently, development of new electrical material with high energy density and cycling stability is very important.

Manganese oxide has gained considerable attention as a lithium ion battery electrode material because of its high capacity, environmental compatibility and low cost [27]. So far,

there are many synthetic procedures for producing MnO_2. The most popular ways of synthesizing the material include (a) reducing MnO_4^- by using reducing agent such as N_2H_4, carbon, ethanol or ascorbic acid, (b) oxidizing Mn^{2+} by using oxidizing agent such as $S_2O_8^{2-}$, H_2O_2, and O_2[28]. The electrochemical performance of the cell heavily depends on the shape and particle size of the material[28]. Accordingly, using M13 phage biotemplating can be a very attractive solution for producing MnO_2. Generally, production of MnO_2 can be achieved through a procedure of phase transformation. It has three possible confirmations (α,β, and γ) which are temperature dependent and require the presence of cations. Figure 5.1 summarizes the conformational change of MnO_2[28].

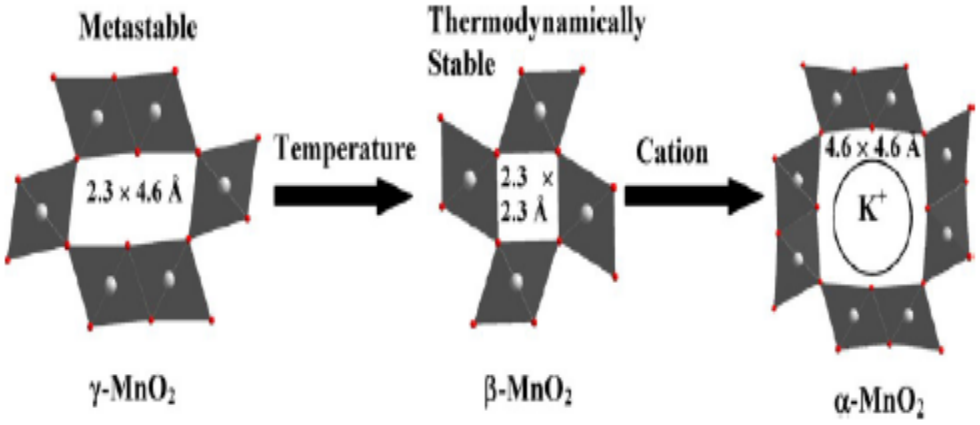

Figure 5.1 Phase transformation of MnO_2 in various conditions.[28]

Hydrothermal reaction of the material is the most desired synthetic procedure for preparing MnO_2. But, this process is usually time consuming so it can't be a very good candidate for synthesizing biotemplated materials[28]. Instead of synthesizing MnO_2 directly, we could synthesize the material from MnOOH at room temperature. By doing this, preservation of the material morphology also can be achieved.

Besides, MnO_2 has a lot of other practical applications and it can be used as a capacitor material and a catalyst for CO oxidation as well as a catalyst for Lithium air batteries. The applications of the MnO_2 material and descriptions of which qualities are desired for certain applications are covered briefly in the next sections.

Lithium ion battery electrode material

Although MnO_2 has high theoretical capacity, it has very low conductivity and high volume expansion which limit its use as an electrode material for lithium ion battery[31]. These issues were resolved recently by Li's group with using Graphene/Polymer/MnO_2 composite[31]. In their work, they used *in situ* polymerization of EDOT on graphene sheet and thereafter triggered the growth of MnO_2 on the graphene/EDOT composite. Figure 5.2 summarized the process of producing the MnO_2/EDOT/Graphene composite.

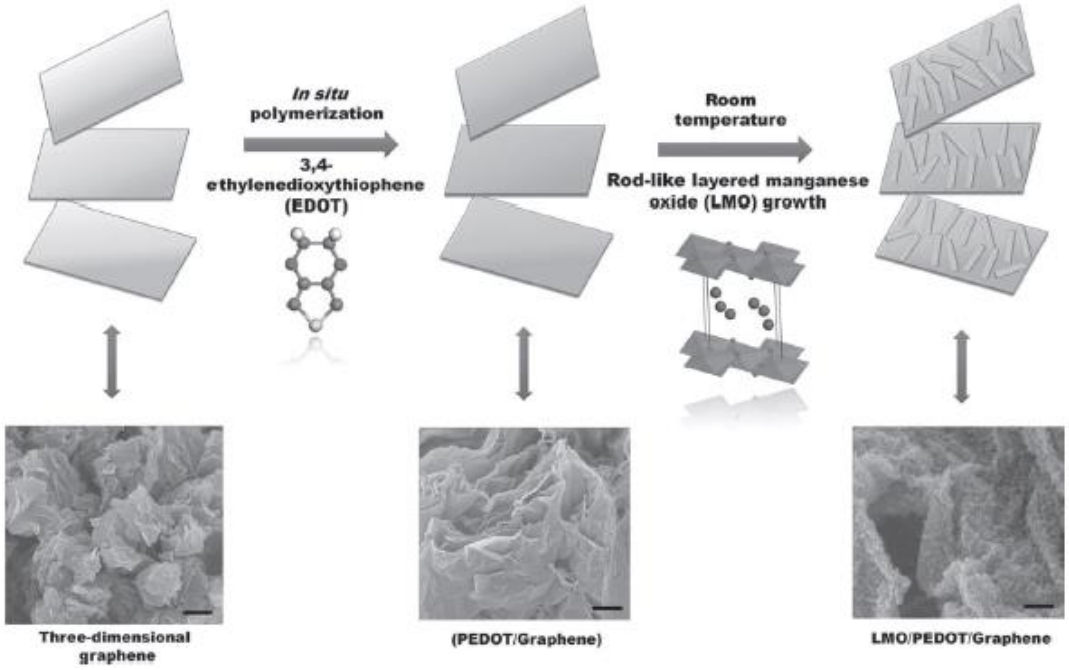

Figure 5.2 Schematics of producing MnO_2/EDOT/graphene composite [31]

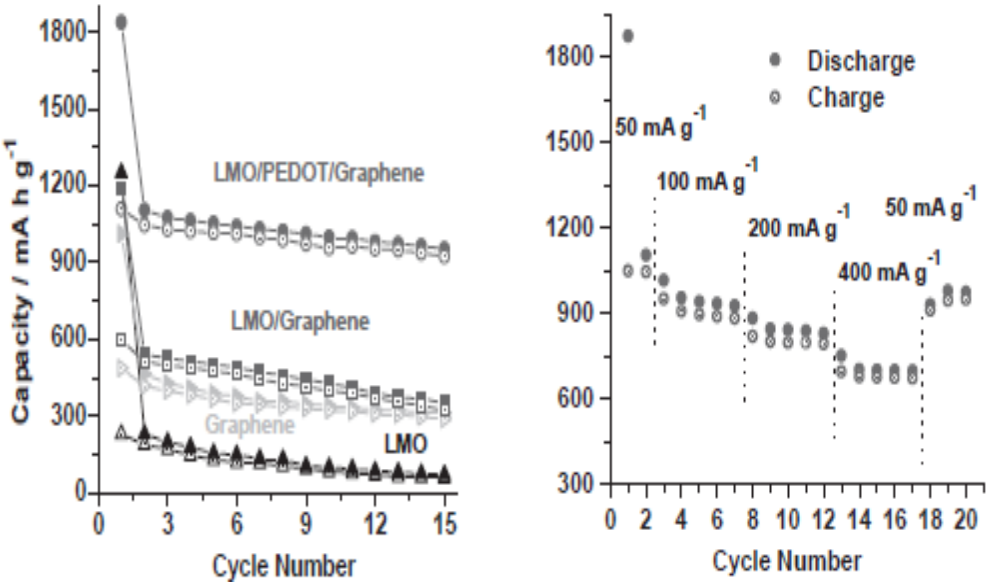

Figure 5.3 Electrochemical performance of the material .[31] Right graph shows the discharge capacity of the material at current density of 50mAh/g and the left graph shows the capacity of the material at various current density.

In their experiment, the MnO_2 product displayed excellent capacity retention even after 15 cycles with a capacity of 1000mAh/g, the highest value known so far as shown in figure 5.3[31]. Furthermore, for solving the issue of low conductivity, they used an alternative approach to grow MnO_2 on carbon nanotubes (figure 5.4). However, this strategy did not show a promising performance since the capacity of MnO_2/EDOT/graphene composite sharply decayed to 500mAh/g after 15 cycles[31].

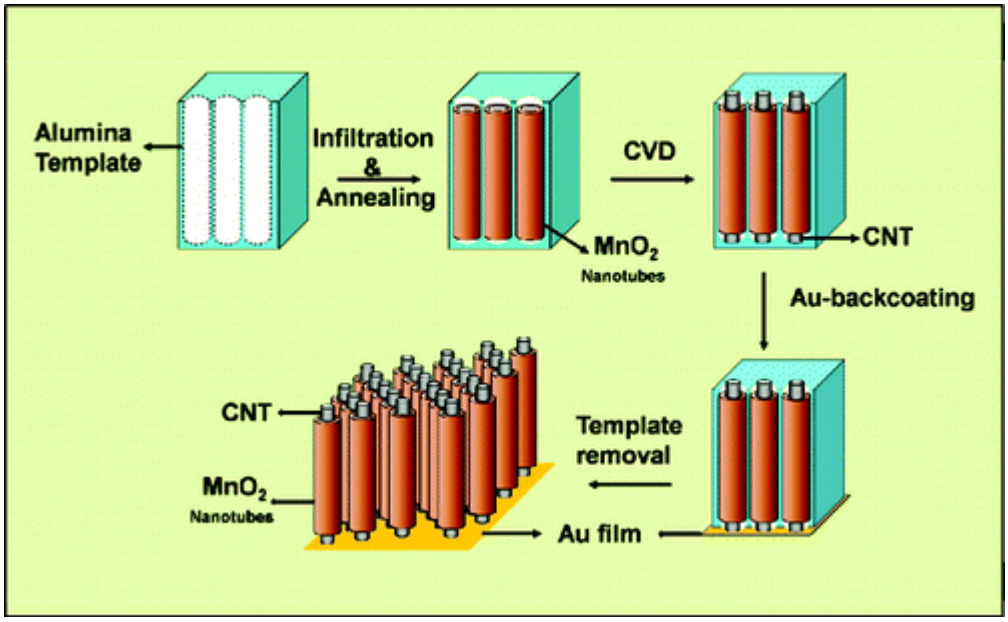

Figure 5.4 Fabrication of coaxial carbonanotube/MnO2 array electrode[32]

In summary, many recent reviews have confirmed that MnO_2 can be an attractive electrode material for Lithium ion battery once the low conductivity issues are overcome.

Catalyst

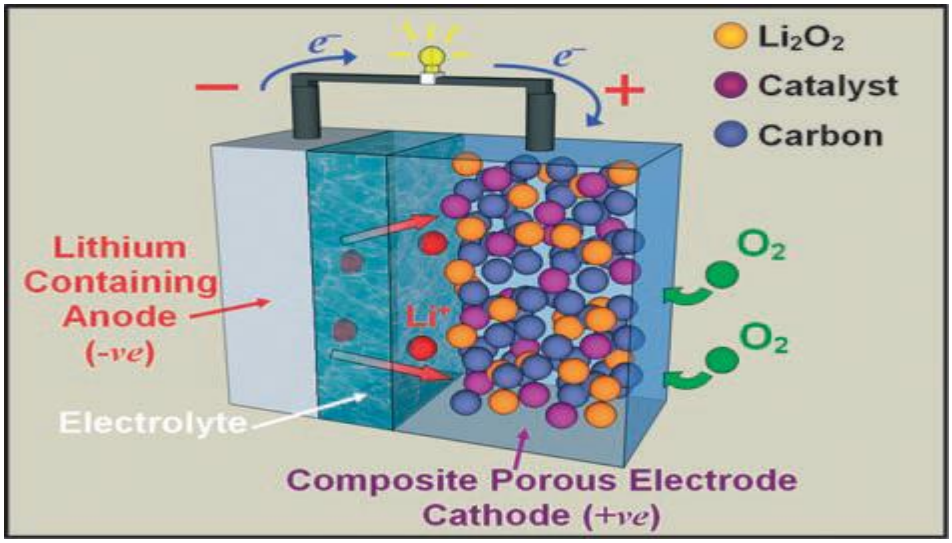

Figure 5.5 Schematic of working principle of Li/O_2 battery[33]

Lithium air battery is drawing a lot of attention due to its high energy density. Till now, it contains the highest energy density among all other batteries[34]. In 2010, there are 14 Lithium-air battery articles being published. Now, many researchers are working on Lithium-air battery trying to increase its capacity and efficiency[34]. Lithium air battery is a good candidate as a power source for electrical vehicle, where high energy density energy source is crucial [34]. For good electrochemical performance of Lithium air battery, good catalyst is necessary. Figure 5.5 summarizes the general mechanism of catalyst in a Lithium air battery. Figure 5.6 summarizes energy density of the lithium air batteries compared to other power sources.

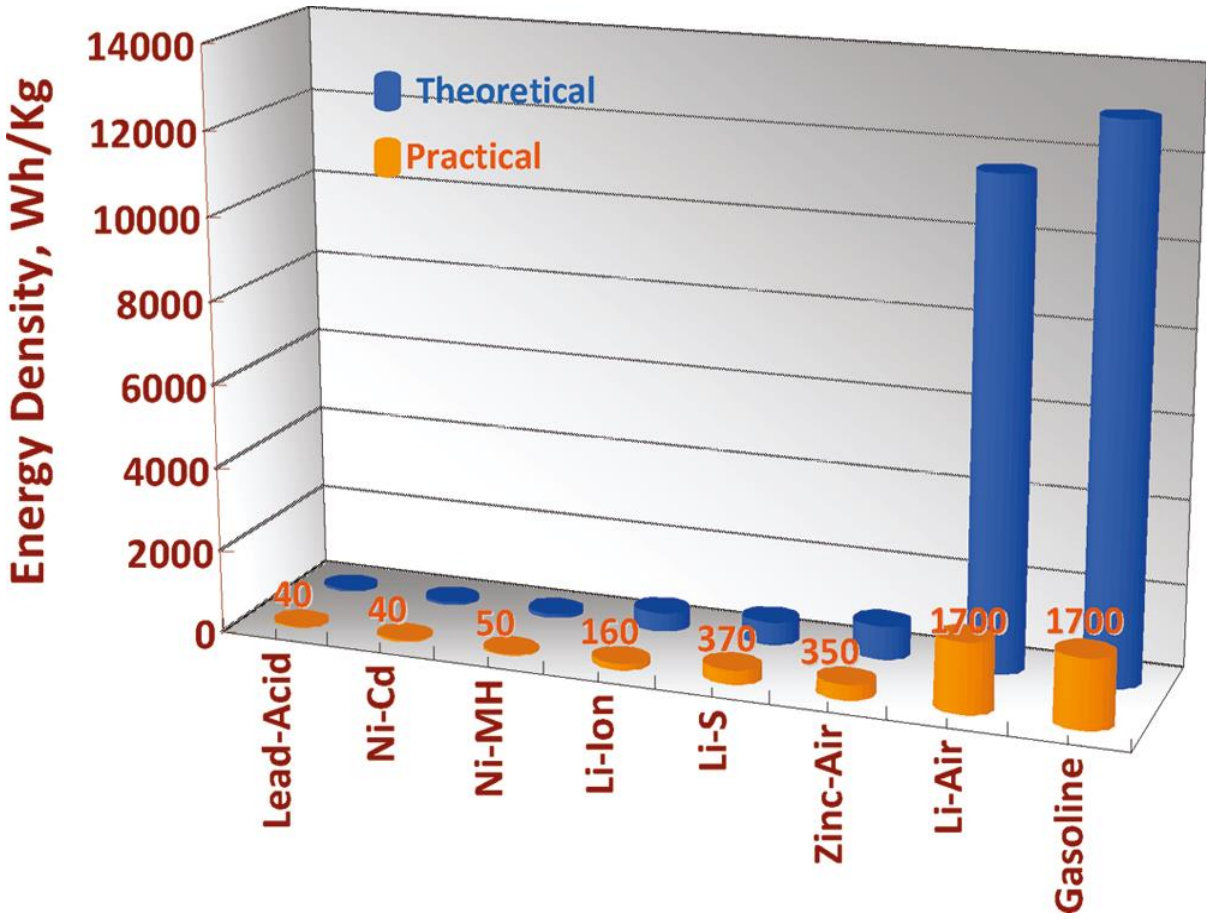

Figure 5.6 The gravimetric energy density of the batteries in comparison to gasoline [34]

Catalyst plays a very important role in determining the performance of Lithium air batteries. So far, Co_3O_4, Fe_2O_3, MnO_2, and CuO have been investigated as the common catalyst materials for Lithium air battery[34]. The potential of MnO_2 as a catalyst material for Lithium air battery has been proving in a recent research work showing superior catalytic performance of nano MnO_2 over other manganese oxide catalysts [33]. As for the phase, alpha MnO_2 elicited the best performance over beta and gamma MnO_2[33,34]. From this result it was concluded that the MnO_2 can be a cheap and efficient catalyst material for Lithium air battery.

5.2 Experimental

5.2.1 Preparation of M13-MnO_2 nanowires

MnO_2 was made by a simple precipitation method. Briefly, manganese sulfate monohydroxide (1g, sigma Aldrich) was dissolved in 90 mL of distilled water and the solution was stirred in a constant speed (250 rpm) for 10 minutes. The resultant solution was then mixed with 10mL of M13 phage solution (10^{13} CPU/mL) and the phage- manganese sulfate solution was stirred constantly in room temperature for 24 h. Next, 4.5mL of 2.5M sodium hydroxide solution was added to the mixture. After 10 seconds, 20 mL of 2% hydrogen peroxide solution was added slowly by using a burette, which is shown in figure 4.2.

Figure 5.7 M13- MnO_2 nanowires

Subsequently, the mixture was then formed black precipitate and the solution was centrifuged in 5000 rpm for 30 seconds (figure 5.7). The resultant mixture was centrifuged and washed 10 times with distilled water and then with 70% ethanol. The black precipitate was dried at 100^{o}C oven for 24 hours. The black precipitate was calcined at 200^{o}C for 3h afterwards. The resultant compound was grinded by hands for characterization tests.

5.2.2 Material characterization

The product obtained from the procedure was analyzed with X-ray diffraction using Cu k α radiation. The surface morphology of the product was examined with Scanning Electron Microscope (SEM, Leo-1530, Zeiss).

5.2.3 Electrochemical measurement

The electrochemical performance of M13- MnO_2 composite samples was tested using coin type cell (CR2032). Each cell composed of a lithium metal anode and a Mn_2O_3/acetylene black/polyvynylidene fluoride (PVDF, Kynar, HSV900) cathode. The cathode was made by carefully mixing the 70 wt. % M13-Mn2O3 composite, 20 wt. % acetylene black as conductive agent and 10 wt.% PVDF as a binder. The resultant mixture was painted on a copper foil with 1cm diameter and the foil was dried in a vacuum oven overnight at 60^oC. The material loaded on the each electrode was about $3mg/cm^2$. Thereafter, the cell was tested on galvanostatically on a Neware multichannel battery tester between 0.01V-3V *vs* Li^+/Li at current density of 0.1C.

5.3 Results and Discussion

5.3.1 XRD characterization

The XRD results are summarized in figure 5.9 and 5.10. From the figures it is revealed that the material was in good match with MnO_2 confirming that we can successfully produce MnO_2 with this method.

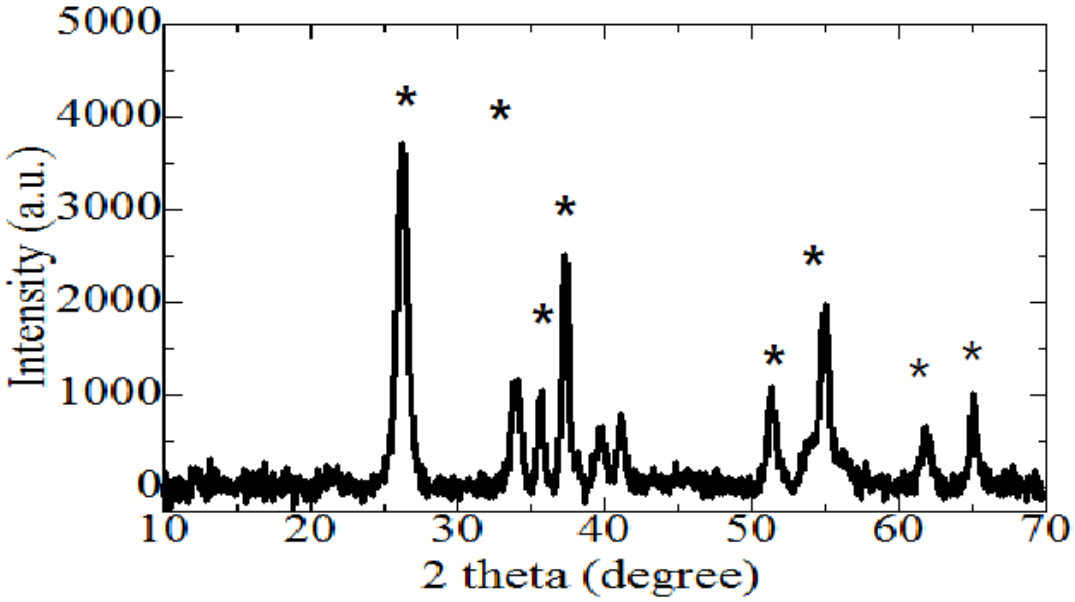

Figure 5.8 XRD pattern of the product before calcination. * represent the reference peaks for MnOOH. Unlabeled peaks are mixture of Mn_2O_3 and MnO_2

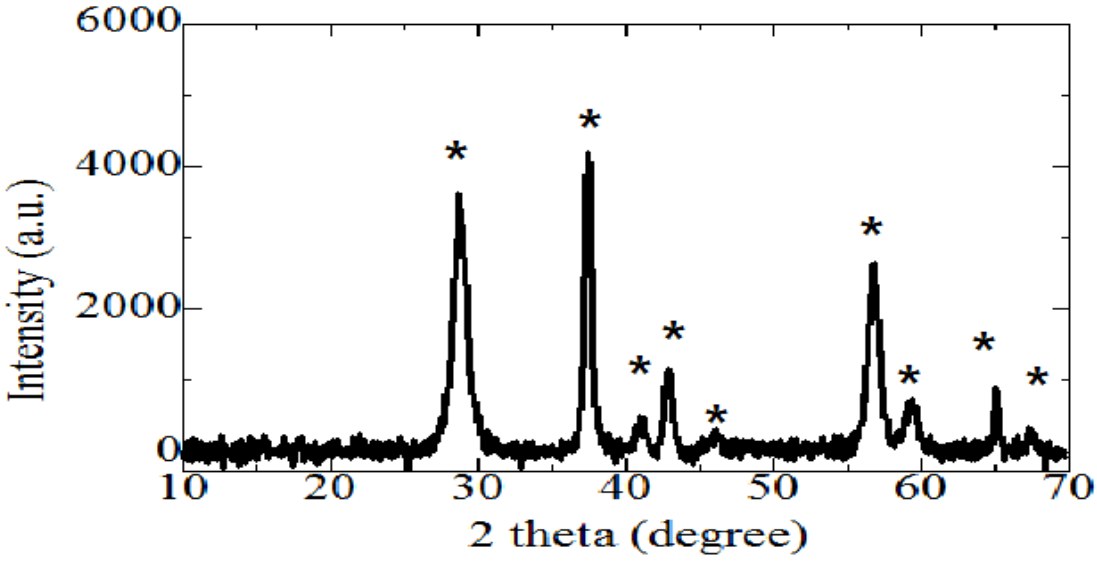

Figure 5.9 XRD pattern of the product nanowires after calcination. * represent the reference peaks for MnO_2.

From figure 5.8 we ascertain that addition of hydrogen peroxide produced manganite, MnOOH. However, after the calcination at 200^{o}C, the manganite was transformed to MnO_2. Transformation phenomenon and the chemistry behind it will be discussed further in the next section. The synthesis of MnO_2 takes place through synthesis of MnOOH. Synthesis and analysis of the MnOOH will not be discussed further in this section as all the relevant information was described in section 4.4.1.

After the production of MnOOH, the material was calcined at 200 ^{o}C for 2h to transform MnOOH into MnO_2 nanowires. Figure 5.10 shows that the material corresponded to MnO_2 pattern. Since the material had very broad peak, it is very hard to define its phase. Based on literature, it's speculated that the material seemed more likely to be beta MnO_2. But, the possibility of alpha phase form can't be excluded[33]. Nevertheless, the XRD data proved that the material was indeed MnO_2.

Figure 5.10 Overall summary of the reaction

After confirming the product, I checked the material for its surface morphology by using SEM. The SEM image showed fine nanowire surface morphology without aggregation. Figure 5.11 and 5.12 summarize the surface morphology of the material.

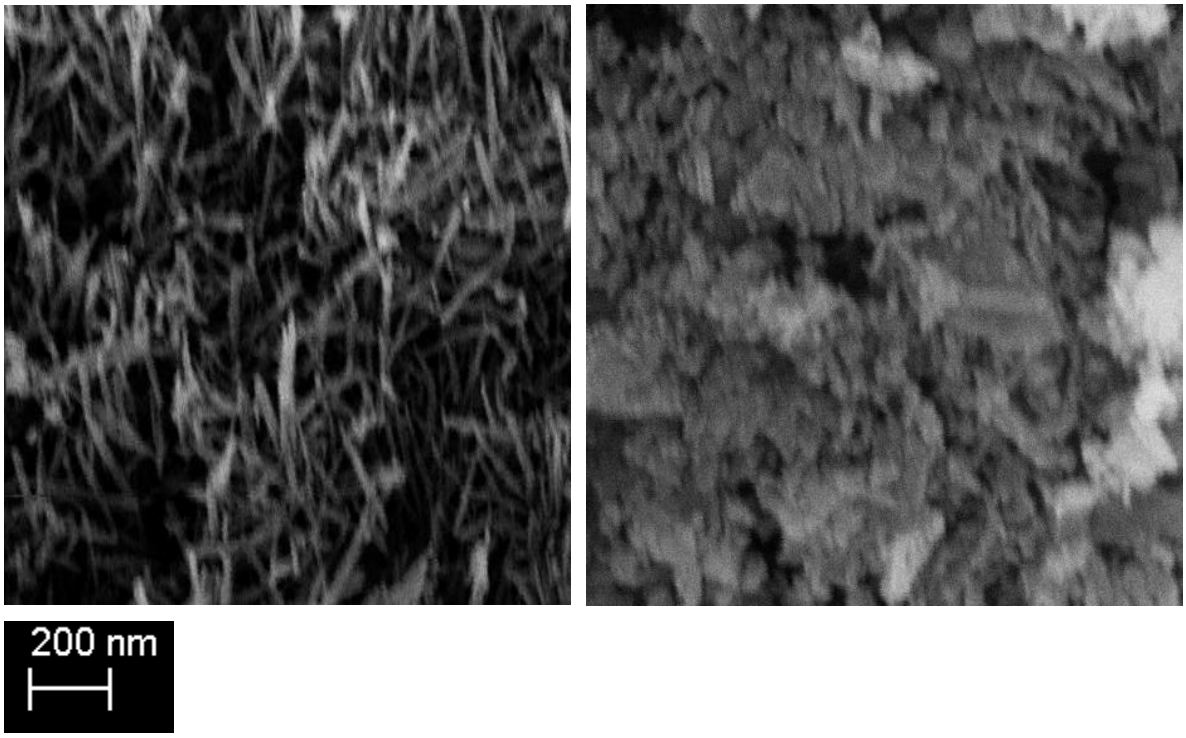

Figure 5.11 Product before calcination with M13(left) and without M13 (right). Both of the products were MnOOH.

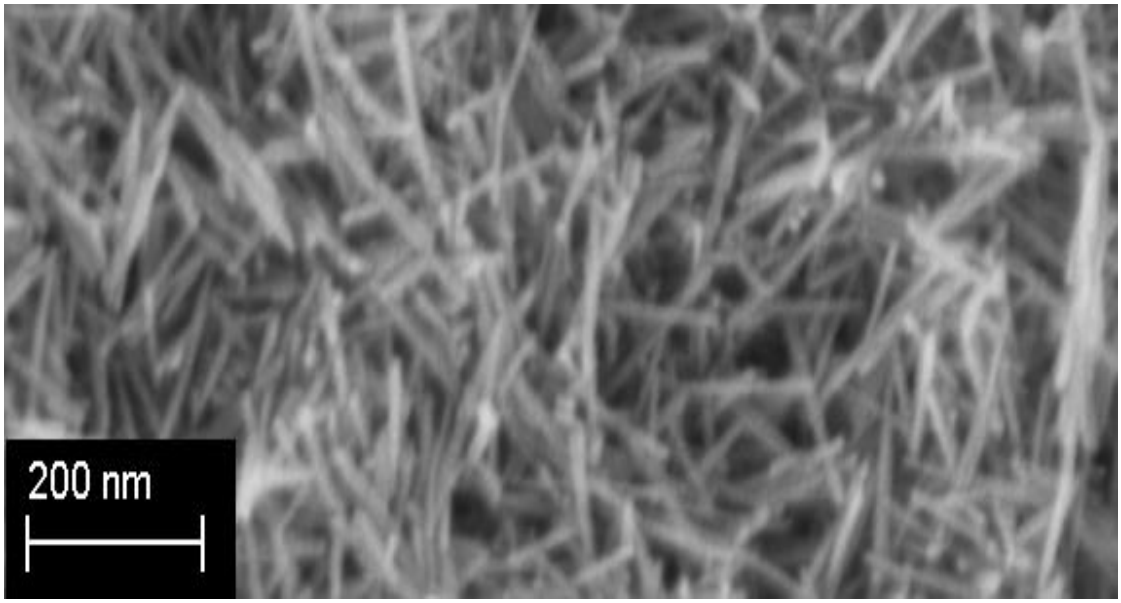

Figure 5.12 Product after calcination. The product was MnO_2.

As Figure 5.12 reveals, the MnO_2 had a shape of nanowires with a diameter of about 10nm and a length of 600nm. This nanowire morphology provides numerous benefits for improving performance of battery via increasing in surface area and easy of lithium ion intercalation. Additionally, the material was tested for the electrochemical performance. As mentioned before, MnO_2 can be used as a negative electrode material for lithium ion battery due to its good surface morphology and small particle size. Figure 5.13 displays the electrochemical performance of the material at current density of 0.1C.

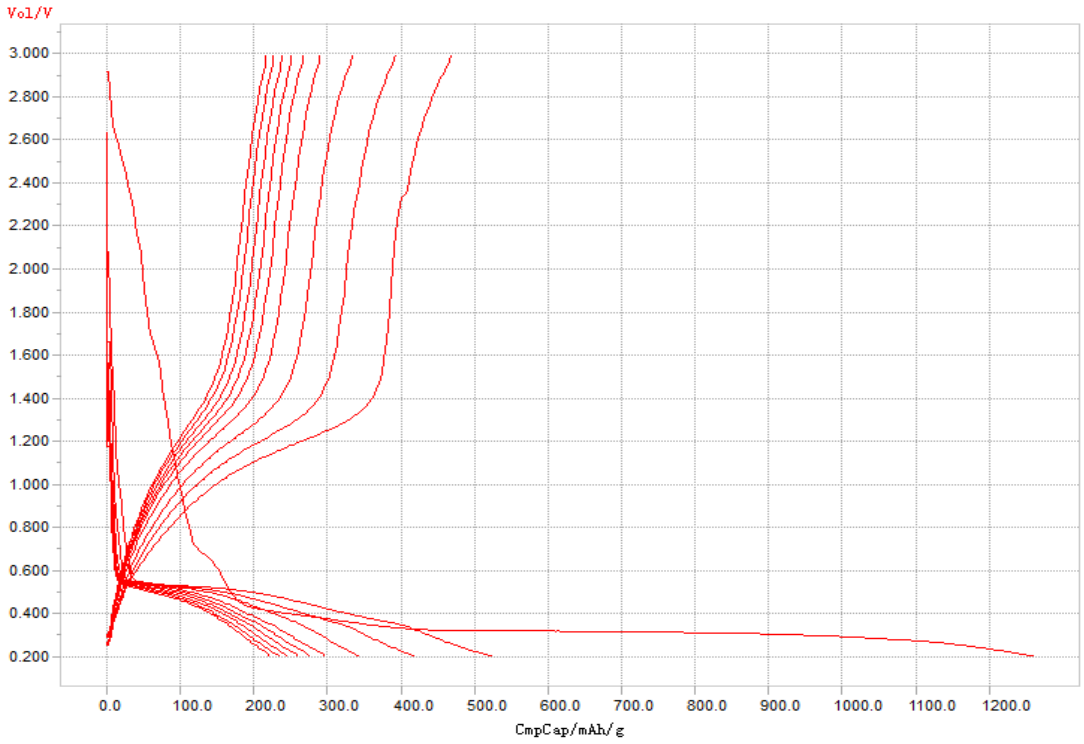

Figure 5.13 Capacity retention of MnO_2 at 0.1C

As the figure above shows, the material had very poor capacity retention after the first discharge with a capacity of 530mAh/g, which is only about 40% of the first cycle. Just after 5 cycles, discharge capacity of the material became lower than 300mAh/g.

Although the material had very high initial capacity of 1200mAh/g, the material failed to maintain its initial discharge capacity. The most probable explanations for the result are that the material had poor conductivity and high volume expansion during the battery operation [31] . Although the material had good surface morphology, lacking of conductive additive makes it a very poor battery material. The Belcher's group has solved this issue by applying genetic engineering. In their work, they changed the structure of pIII protein so that M13 phage possessed binding affinity to single walled carbon nanotubes [2,3,35]. However, applying genetic engineering needs a lot of resources and expertise in the field and bioengineering research in this field has not been attempted since then. The Lithium ion intercalation reaction on the material can be summarized as equation 4 below [32]:

$$MnO_2+4Li^+ + 4e^- \leftrightarrow Mn + 2Li_2O \quad (1) \qquad (4)$$

$$4Li \leftrightarrow Li^+ + 4e^- \quad (2)$$

$$MnO_2 + 4Li \leftrightarrow 2Li_2O + Mn \quad (3)$$

The present synthetic procedure successfully produced MnO_2 nanowires. Although its application as an electrode material for battery is limited, the material can be used for other applications such as catalyst for Lithium air battery. Due to its high surface area to volume ratio, the material can be a very good catalyst material.

5.4 Summary

It is possible to synthesize nanosized MnO_2 material by using M13 template. The material displayed very good surface morphology with a diameter of 10nm and a length of 600nm. The material did not show good capacity retention once it was used as an electrode material for Lithium ion battery. Further investigation is needed to find suitable applications for MnO_2 material.

Chapter 6
Synthesis of M13-Mn_3O_4 nanocomposite

6.1 Overview of Mn_3O_4

Mn_3O_4 is generally used as the negative electrode material for lithium ion battery due to its high capacity and environmental benignity and low cost. The theoretical capacity of Mn_3O_4 is 936mAh/g, which is about three times higher than that of graphite (372mAh/g)[36] , the most commonly used negative electrode material for Lithium ion battery.

Many metal oxides such as FeO, NiO, Co_3O_4, and Fe_3O_4 are promising candidates for negative electrode materials for Lithium ion batteries[36]. Presently, these materials are studied extensively and some good research progresses have been reported. For example, Ban *et al.* showed an enhanced performance of Fe_3O_4 in their recent work [36]. Unlike other anode materials, there are not many papers regarding Mn_3O_4 application. Insufficient publication on Mn_3O_4 is probably due to its low conductivity and high volume expansion after cycling that limit its use as an electrode material[36]. Similar to Mn_3O_4, most manganese oxides suffer from very low capacity retention. So far, the best data only showed 60% columbic efficiency after the first cycle[36]. This issue is very hard to resolve and it is still one of the greatest challenge for material chemists.

While many other manganese oxides such as Mn_2O_3 and MnO_2 are black in color, Mn_3O_4 is brown. Synthesis of Mn_3O_4 usually involves either (1) high temperature or (2) organic solvent[36,37]. Since M13 phage can stand neither of them, a new synthetic procedure is needed to produce Mn_3O_4 nanocomposite. In my experimental design and procedure, the synthesis of Mn_3O_4 could be carried out via aqueous synthesis and under room temperature

condition. With my protocol, the structure of M13 phage can be preserved while production of Mn_3O_4 is achieved. After the synthesis, the material was tested for electrochemical performance.

This chapter is composed of 4 main subsections: literature review on the material, experiments, results and discussion, and conclusion. Figure 6.1 shows M13-Mn_3O_4 nanocomposites.

Figure 6.1. Mn_3O_4 nanocomposite.

6.2 Literature review: applications of Mn_3O_4

As mentioned in the introduction, there are not many research papers on Mn_3O_4 battery for Li-ion battery applications. In this section, I attempt to cover the very important research advances.

Sponge-like Mn_3O_4

Aburna's group has synthesized sponge-like Mn3O4 for negative electrode material for Lithium ion battery[36]. Although the material was a micron-size scale, the material showed excellent capacity retention at a high current rate of 0.25 C. The material maintained high capacity of 800 mAh/g after the 40 cycles. Figure 6.2 showed the SEM picture of the material.

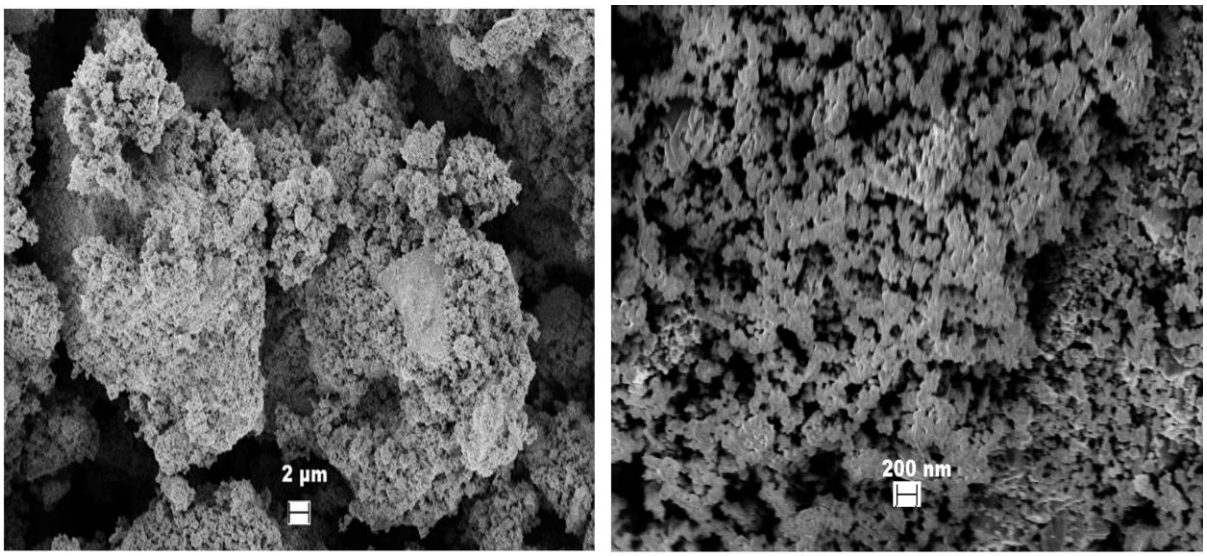

Figure 6.2 SEM picture of spongelike Mn_3O_4[36].

One thing to note from this work is that the material synthesis was done in low temperature compared to other Mn_3O_4 synthesis procedure such as Co doping and or organic synthesis. Besides, this synthetic procedure is rather simpler than other methods[36]. The material demonstrated very good capacity retention and had very high discharge capacity. On the other hand, this material showed very low columbic efficiency of 60% after the 1st cycle [36] due to low conductivity of the material. Although it used 20% wt. of the carbon additives

to slurry, the low conductivity issue of the material was still not fully overcome[36]. Nevertheless, this is the one of the best result achieved for Mn_3O_4 synthesis.

Mn_3O_4-graphene hybrid

Yi Cui's group has produced Mn_3O_4-graphene hybrid material for Lithium ion battery[37]. As mentioned before, Mn_3O_4 suffers from low conductivity limiting its use as a battery material. In this study, Mn_3O_4 had conductivity of 10^{-7}-10^{-8}S/cm[37], which is the key reason for its low capacity retention. Even with Co dope, Mn_3O_4 can only manage to give capacity of 400mAh/g. However, Mn_3O_4-graphene hybrid showed excellent capacity of ~900 mAh/g, the highest known value so far[37].

Graphene is now considered as the next new wonder material. Its usage is not solely limited to battery application but medicine, drug delivery, electrics, optics, and even fiber material [37]. The Cui's group suggested that graphene template approach can be extended further to insulate electrode material for Lithium ion battery. Figure 6.3 summarizes synthetic procedures of making graphen-Mn3O4 nanocomposites.

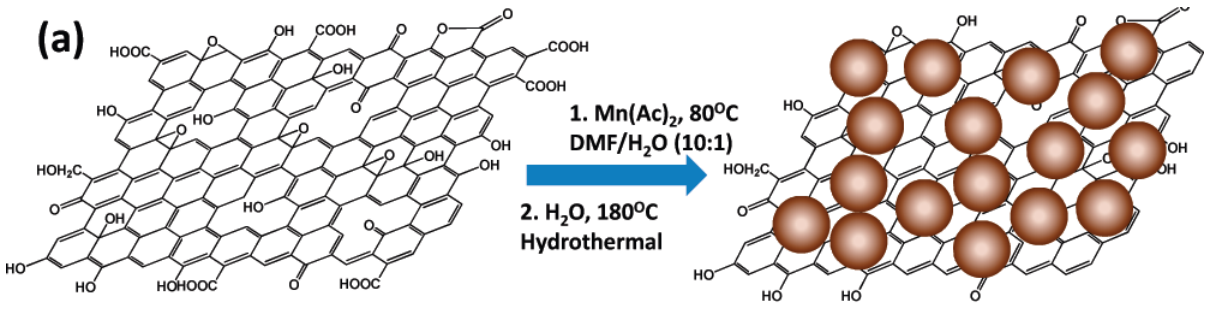

Figure 6.3 Graphen-Mn3O4 hybrid[37]

Mechanism of the main reaction is the same as M13 phage-manganese oxide since graphene oxide has carboxyl group on the surface allowing the charge interaction between manganese ion and graphene oxide. When the reaction is completed, graphene- Mn_3O_4 hybrid was produced. The material can also stand high current density up to 1600mAh/g, and yielded capacity recovery once the current density decreased[37] to 40 mAh/g. This data is very promising as free Mn3O4 can manage to have discharge capacity of 200mAh/g after several cycles. However, the material synthesis was very complicated and time consuming and requires organic solvent. Moreover, graphene oxide which acts as a conductive template material for Mn_3O_4, is a very expensive material. Even if graphene is considered as the next wonder material, it will be too expansive to use as a commercial battery material. It is suggested that Mn_3O_4 may have a good value as a negative electrode material for Lithium-ion battery since it's a cheap, abundant, and environmental friendly material.

Cobalt-doped Mn_3O_4

West's group solved the low conductivity issue by doping Cobalt to Mn_3O_4. In this study, the researchers have managed to maintain capacity of 400 mAh/g, which was twice as high as undoped Mn_3O_4[38]. Although Cobalt-doped Mn_3O_4 had much smaller capacity than graphene- Mn_3O_4 hybrid, it was the first work performed to improve the conductivity of Mn_3O_4[38].

6.3 Experimental

6.3.1 Preparation of M13-Mn_3O_4 nanowires

Mn_3O_4 was made by a simple precipitation method. Manganese sulfate monohydroxide (2g, sigma Aldrich) was dissolved in 90mL of distilled water and the solution was stirred at a constant speed for 10 minutes. The resultant solution was then mixed with 10 mL of M13 phage solution ($1*10^{13}$ CPU/mL) and stirred constantly at room temperature for 24 h.

Next, 4.5 mL of 2.5 M sodium hydroxide solution was added to the mixture and stirred for 10 seconds. Thereafter, 1.4mL of 30% hydrogen peroxide solution was added instantly with an automatic pipet.

Shortly, the mixture was formed a brown-black precipitate and then it was centrifuged at 5000 rpm for 30 seconds. The resultant mixture was washed 10 times with distilled water and then with 70% ethanol for once. The black precipitate was dried at 100^oC in an oven for 72 hours. The resultant compound was grinded by hands and subjected for characterization tests.

6.3.2 Material characterization

The structure obtained from the procedure was analyzed with X-ray diffraction using Cu kα radiation. The surface morphology of the product was investigated by using Scanning Electron Microscope (SEM, Leo-1530, Zeiss).

6.3.3 Electrochemical measurement

The electrochemical performance of M13- Mn_3O_4 composite samples was tested using coin type cell (CR2032). Each cell composed of a lithium metal anode and a Mn_3O_4/acetylene black/polyvynylidene fluoride (PVDF, Kynar, HSV900) cathode. The

cathode was made by carefully mixing the 70 wt. % M13- Mn_3O_4 composite, 20 wt. % acetylene black as conductive agent and 10 wt.% PVDF as a binder. The resultant mixture was painted on a copper foil with 1cm diameter and the foil was dried in a vacuum oven overnight at 60^{o}C. The material loaded on each electrode was about 3mg/cm^{2}. The cell was tested on galvanostatically on a Neware multichannel battery tester between 0.01V-3V *vs* Li^{+}/Li at C-rate of 0.1C.

6.4 Results and Discussion

6.4.1 XRD characterization

The XRD result as summarized in figure 6.4 confirmed that the material was indeed Mn_3O_4. The figure showed that the material was in a good match with Mn_3O_4 indicating the method can successfully produce Mn_3O_4

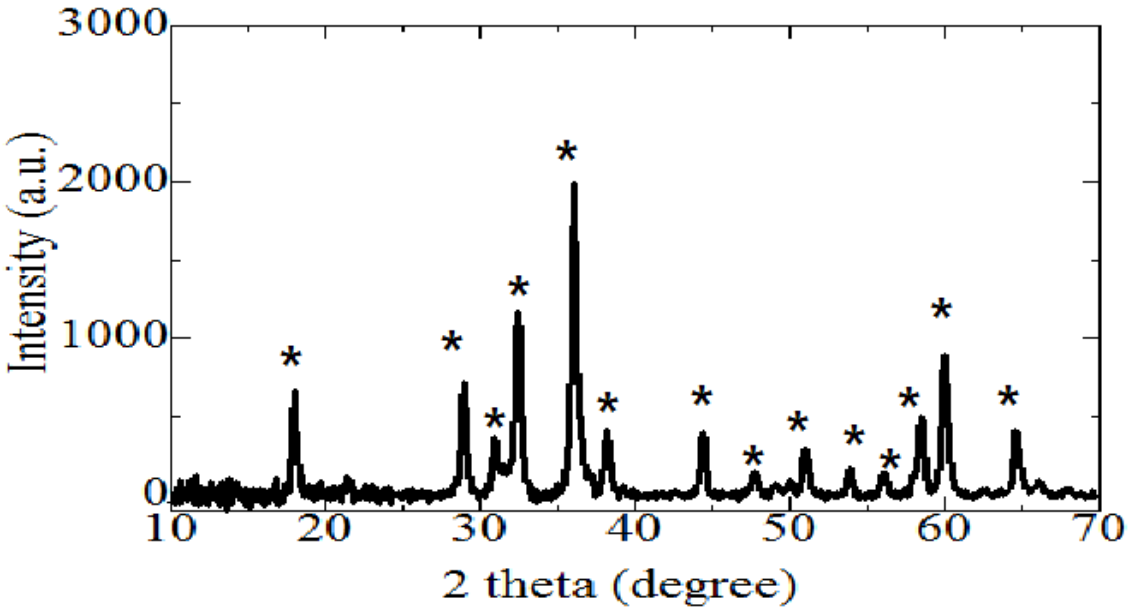

Figure 6.4 XRD pattern of the product. * represents the reference peak for Mn_3O_4.

The mechanism of Mn_3O_4 formation can be summarized[39] in equation 5:

$$Mn^{2+} + 2OH^- \rightarrow Mn(OH)_2 \quad (5)$$

$$4Mn(OH)_2 + O_2 + 2H_2O \rightarrow 4Mn(OH)_3$$

$$Mn(OH)_2 + 2Mn(OH)_3 \rightarrow Mn_3O_4 + 4H_2O$$

The reaction can be completed without presence of H_2O_2 as the equation described above. However, addition of hydrogen peroxide can speed up the reaction. Based on this result, it is confirmed that the current procedure offers a fast and easy method for synthesizing Mn_3O_4 material at room temperature.

6.4.2 Surface morphology and further characterization

Although XRD data confirmed that the material was Mn_3O_4, its surface morphology was still examined. According to Terascon's paper, the surface morphology and particle size are very important in defining application of the material [21], especially for Lithium ion battery application as Lithium ion intercalation is the most desired quality. Figure 4.5 is the SEM image of the M13-Mn3O4 material.

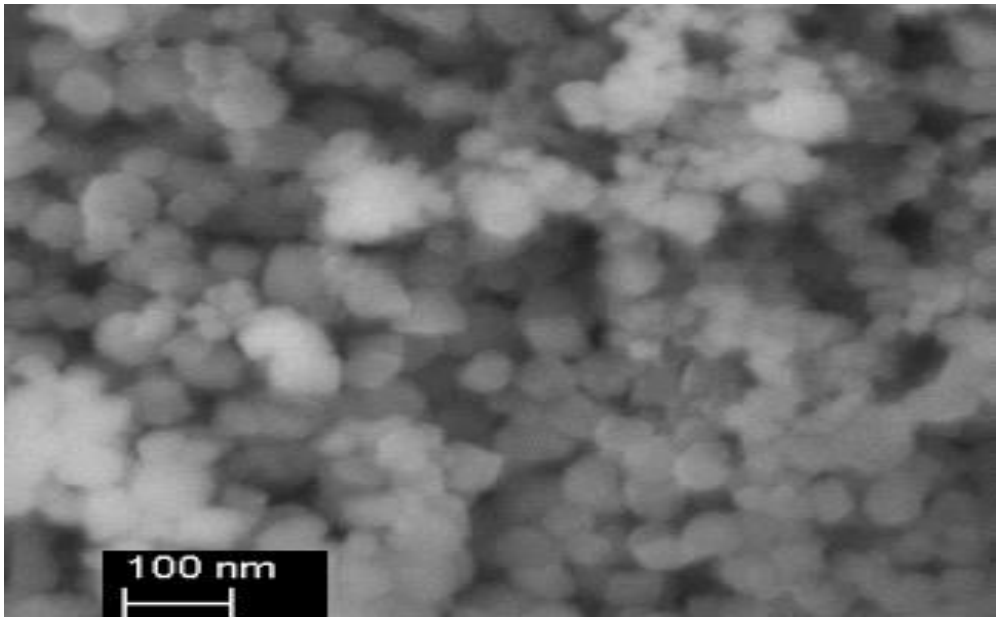

Figure 6.5 SEM image of M13-Mn_3O_4 nanowire

From this figure, nanowire morphology can't be observed. Unlike other manganese oxide materials, the M13- Mn_3O_4 was small spherical particles with a size of 50nm. In fact, the M13- Mn_3O_4 particles were the smallest among other manganese oxide materials implying the biotemplating does not work in this material. To make sure whether the presence of M13 phage manipulated the surface morphology of the material, control experiment was conducted in which phage and synthesized the material did not used under the same procedure. From this experiment I verified that the product was Mn_3O_4. Subsequently, the surface morphology of the material was investigated with SEM and image was presented in Figure 6.6.

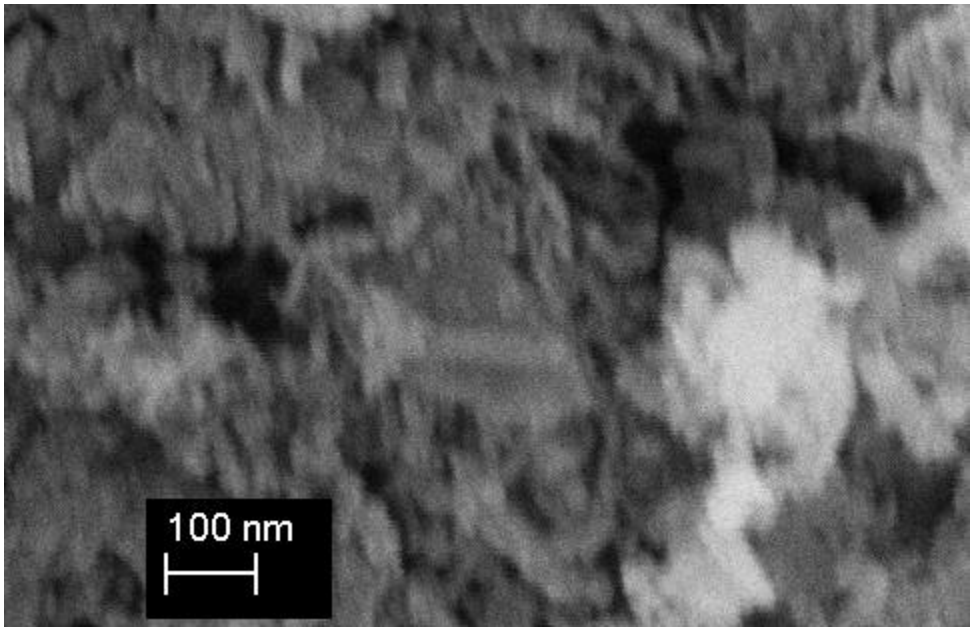

Figure 6.6. SEM image of Mn3O4 without phage.

It is illustrated in Figure 6.6 that the presence of M13 did manipulate the surface morphology of the material. In comparison, the control sample aggregated together and did not present any noticeable surface morphology. Hence, it is concluded that M13 works as a biotemplate material for Mn_3O_4. However, the question why the material did not show the same morphology as the other manganese oxides materials still remains. As mentioned in the previous chapters, nanowire shape was found in Mn_2O_3 and MnO_2 and their particle sizes were about the same as the size of the phage.

Obviously, experimental conditions need to be examined carefully for fully defining the morphology differences. First of all, MnO_2 and Mn_3O_4 were made from MnOOH. During the fabrication procedure, addition of low concentration of hydrogen peroxide at a concentration of 2.1% wt was included. After addition of H_2O_2 in the manganese precursor solution, the hydrogen peroxide was consumed and MnOOH, the black precipitate, was formed instantly.

However, in the Mn_3O_4 fabrication experiment, situation was different. The concentration of hydrogen peroxide was 30%, which was much higher than that in the MnOOH forming environment. Furthermore, addition of hydrogen peroxide was done quickly, the consumption of hydrogen peroxide cannot take place afterwards. It is logical to assume that the remaining hydrogen peroxide played a vital role in making the surface morphology of the material.

The formation of the manganese oxide is very sensitive to hydrogen peroxide concentration. It was observed that once low concentration of hydrogen peroxide was added into the solution manganite (MnOOH) was formed. On the other hand, high concentration hydrogen peroxide formed Mn_3O_4. Similarly, speed of addition played an important role as slow addition tended to form MnOOH rather than Mn_3O_4. Reasons for the differences need to be clarified and but, there is no theoretical backup for the experimental outcomes. So far, it is only an assumption that the addition speed played a crucial role in determining the oxidation status of the manganese oxides.

The hydrogen peroxide, as known from numerous journals, can degrade the protein structure. Fligiel *et al*. in *American Journal of pathology* had showed that the presence of low concentration of hydrogen peroxide can "increase their susceptibility to degradation" of protein[40]. As mentioned in the first chapter, the phage consists of protein and DNA, which can be very sensitive to hydrogen peroxide. In fact, I have confirmed in my previous experiment that 0.1% of hydrogen peroxide in the system can damage the reproducibility of M13 phage. Hence, it is logical that the presence of hydrogen peroxide destroys the phage into parts and the Mn_3O_4, rather than M13 phage, was produced on the top surface protein

debris during the destructive procedure. This also explains why the particle size of the Mn_3O_4 material was not uniform. It is obvious that the size of the particles varied from 2-3nm to 50nm [figure 6.5] . The destruction of phage could create small protein particles and these particles, rather than full size phage, worked as a template.

As mentioned before, the performance of the battery is heavily dependent on particle size and shape. For the case of M13-Mn_3O_4, the particle size is much smaller than other M13-manganse oxides resulted in higher surface to volume ratio. This makes easy for lithium ion to intercalate into the electrode materials.

The electrochemical performance of the material was measured as well. As shown in the previous two chapters, the manganese oxide materials possess very poor capacity retention although the initial capacity of the material was very high. On the contrary, Mn_3O_4 showed excellent capacity retention. Apparently, the low conductivity of the material was very hard to overcome. Figure 6.7 demonstrates the capacity retention of the M13-Mn_3O_4 material. The theoretical capacity of the material was 930mAh/g which was little bit lower than Mn_2O_3.

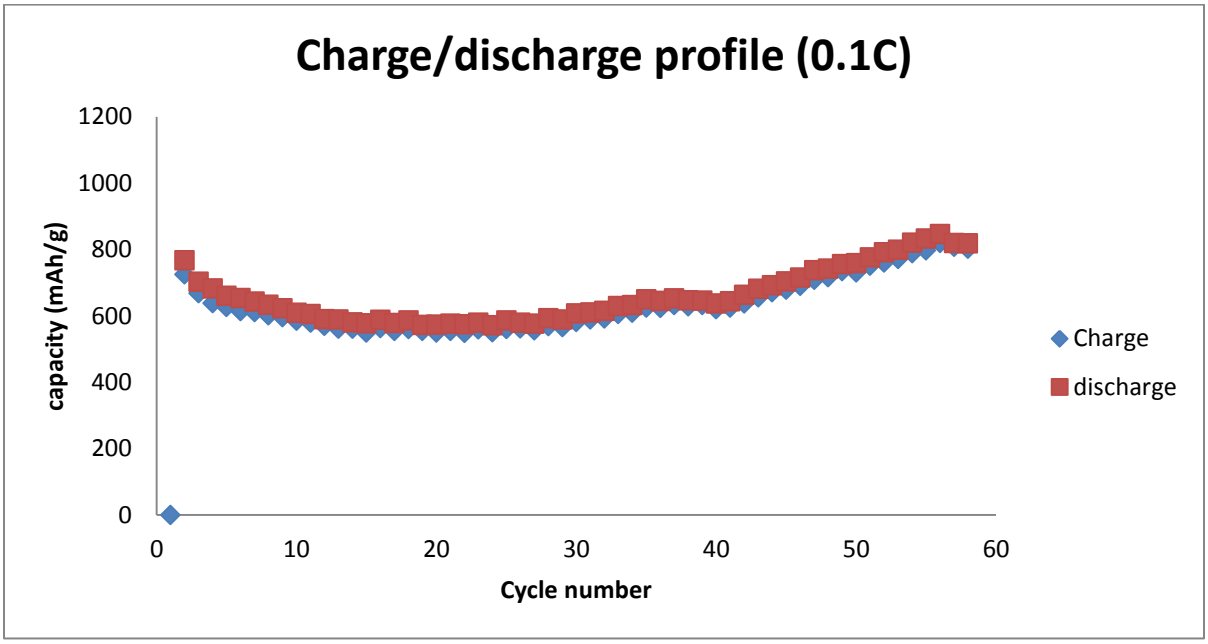

Figure 6.7 Charge and discharge capacity of M13-Mn_3O_4

The M13-Mn_3O_4 material elucidated the discharge capacity of 800mAh/g which is compatible with sponge-like Mn_3O_4. Furthermore, the capacity remained stable up to 60 cycles and it is one of the longest cycle value reported so far. The high capacity and stability of the material makes it possible to use M13- Mn_3O_4 as a high performance negative electrode material for Lithium ion battery. While graphene-Mn_3O_4 displayed excellent capacity retention at 0.05C, M13- Mn_3O_4 gave high capacity retention in high current density.

The material can be synthesized in room temperature through an aqueous synthesis procedure, so the reaction is safe and environmentally friendly. Moreover, production of the material can be completed in less than 2h which is much quicker than any other existing methods.

The low conductivity issue can be solved by using high carbon black content in the slurry. In the experiment, about 20% of the carbon black was added in the slurry, which was much higher than the graphene-Mn_3O_4 hybrid. Since Mn_3O_4 is an insulating material, high carbon content in the sample is needed.

After testing the capacity retention at 0.10C, the material was tested in various C-rate. Figure 6.8 is summarizing the result.

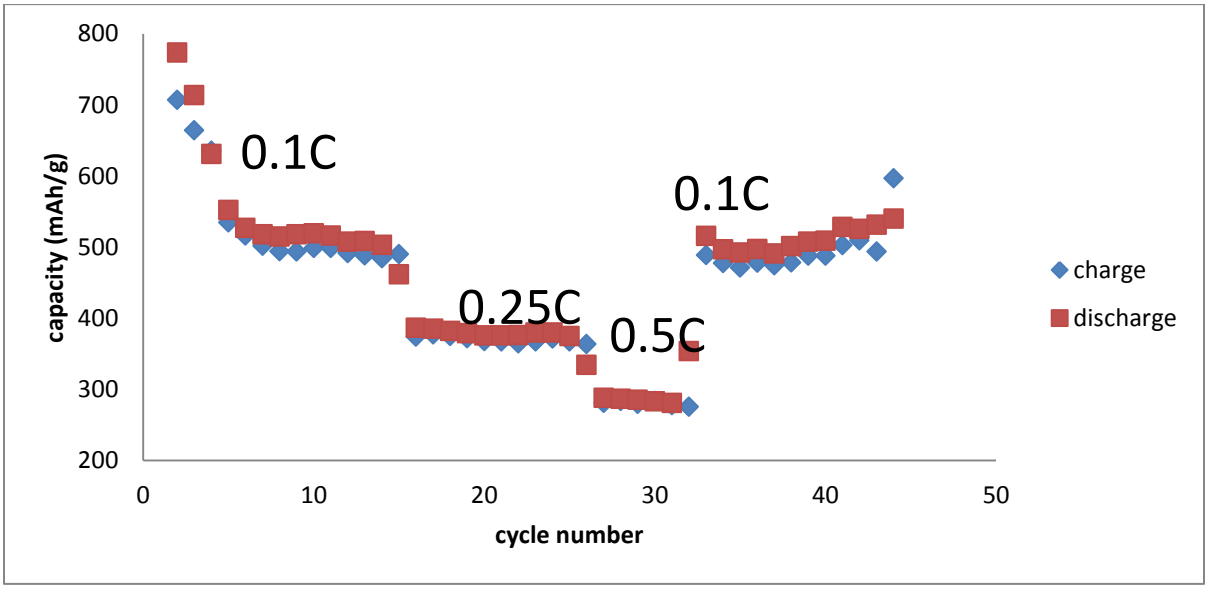

Figure 6.8 Capacity of the material at various current densities

To validate the significance of the material, the Mn_3O_4 material was synthesized without M13 and then tested for electrochemical performance. As expected, the material showed very poor cycling retention even after adding 20% carbon black.

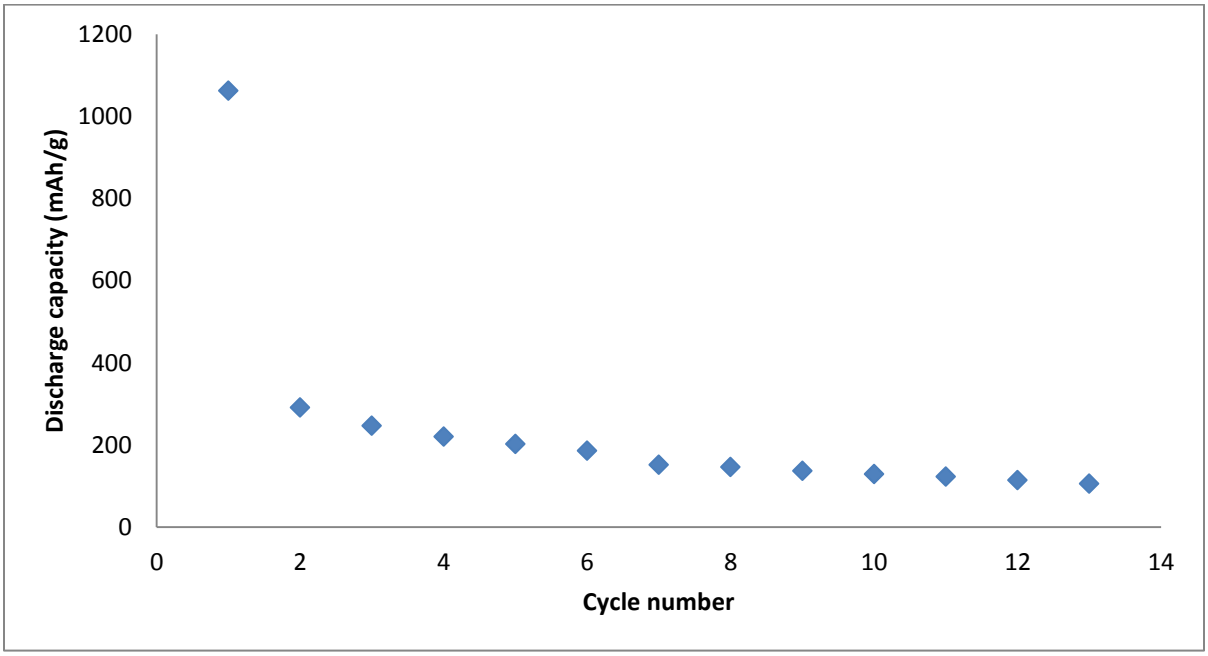

Figure 6.9 Discharge capacity profile of Mn_3O_4 control

As shown above, the addition of M13 phage significantly improved the discharge capacity of the material. When M13 was absent, the material revealed discharge capacity of 200mAh/g after 5 cycles. Furthermore, capacity of the material faded so quickly due to its low conductivity and high volume expansion.

The lithium ion intercalation mechanism on Mn_3O_4 can be summarized as the following equation[37]:

$$Mn_3O_4 + Li^+ + e^- \rightarrow LiMn_3O_4 \quad (1) \qquad (6)$$

$$LiMn_3O_4 + Li^+ + e^- \rightarrow Li_2O + 3MnO \quad (2)$$

$$MnO + 2Li^+ + 2e^- \rightarrow Li_2O + Mn \quad (3)$$

$$Li_2O + Mn \leftrightarrow MnO + 2Li^+ + 2e^-$$

The equation above explains why the first discharge curve showed different pattern as the others discharge pattern.

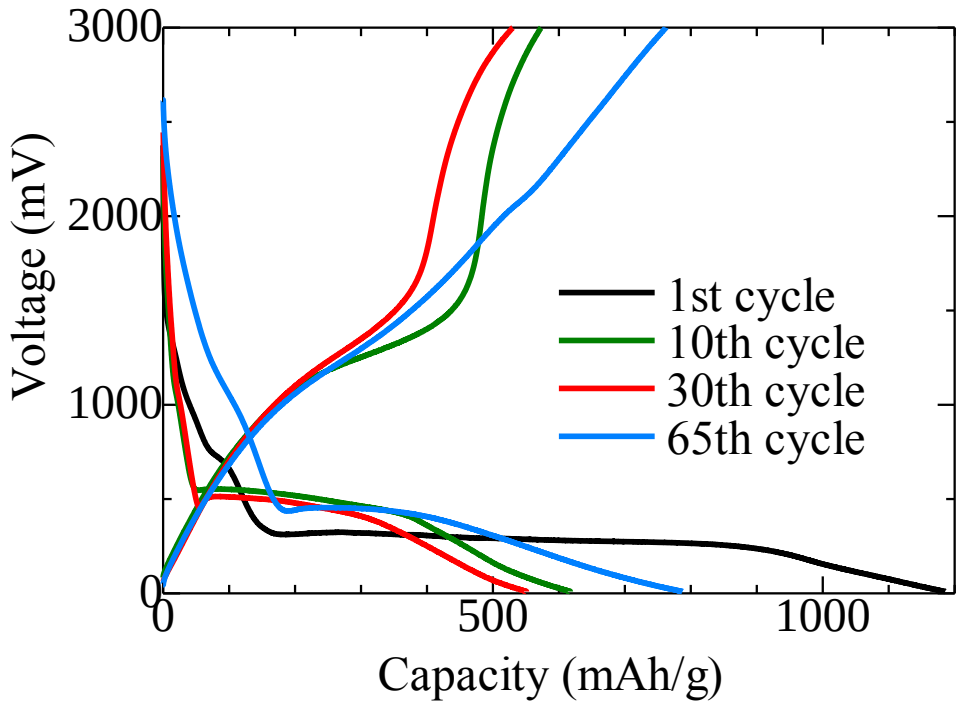

Figure 6.10 Charge and discharge profile of M13-Mn_3O_4

As shown in the figure, the first discharge elicited much higher capacity than others. As well, the first discharge cycles showed much lower voltage than the others. The major difference in discharge characteristics comes from the first 3 lines of the equation. The first three lines in equation 5 are irreversible reactions, and this happens only on the first discharge. Just after the first cycles, the charge and discharge chemistry only follow the last line of the equation, which makes charge and discharge profiles very similar.

From the charge and discharge curve, the material demonstrated as a good negative electrode material for Lithium ion battery. The discharge potential was ~ 0.5V which is

suitable range for negative electrode material. In parallel, the control sample showed very similar charge and discharge profiles except the discharge capacity of the battery dropping very rapidly despite the operating voltage and other general features were very similar.

6.5 Summary

The M13-Mn_3O_4 electrode served as a good anode material for Lithium ion battery. Yet, it needs more research to explain the surface morphology of the materials. The material exhibited much higher capacity than that of graphite (372mAh/g), the most commonly used anode material in industry. In addition, high charge rate testing is required to validate the material. Most work for producing Mn_3O_4 is based on extremely low C-rate, and no work has been conducted for ultra-fast charge and discharge.

Previously, the work was only based on 0.25C meaning it takes 4 hours to charge the material. However, higher charge rate of the materials is desired in order to be practical in industry. If the material is tested in higher charge rate, different pattern will be observed. Still, high theoretical capacity and low cost make it as a very attractive material for lithium ion battery. Therefore, further research of the material is urgently required to satisfy the market demand of new electrode materials.

Chapter 7
Conclusions and Future work

7.1 Production of M13-Mn_2O_3 nanocomposites

It is possible to synthesize M13-MnOOH nanowires at room temperature. The calcination of the material at 700 ^oC can cause the transformation of the material which means MnOOH was transformed to M_2O_3, the material of interest. However, the material had poor capacity retention and the discharge capacity of the material quickly fell to ~300 mAh/g after 5 cycles, which is lower than the theoretical capacity of the graphite. From a recent publication it seems that Mn_2O_3 can hold discharge capacity of 796 mAh/g after 50 cycles implying that the material can serve as an anode material for Lithium ion battery[27]. However, further optimization process is required to enhance the electrochemical performance of the material. Future work should be focused on investigating its usage as a catalyst for oxidation of carbon monoxide and ethylene.

7.2 Production of M13-MnO_2 nanocomposites

MnO2 nanowires can be synthesized successfully by using M13 phage template. It had a diameter of 10nm and a length of only 600nm and the material showed very good surface morphology. The SEM images confirmed that the M13 phage morphology was preserved after fabrication. However, the material did not show good capacity retention once it was used as an electrode material for Lithium ion battery. The discharge capacity of the MnO2 quickly decayed to ~300 mAh/g after 5 cycles. Thus, further optimization is needed to

increase the capacity retention of the material. Furthermore, the material can be tested for other applications such as catalyst for Lithium-air battery.

7.3 Production of M13-Mn_3O_4 nanocomposites

The M13-Mn_3O_4 electrode served as a good anode material for Lithium ion battery. Yet it needs more research to explain the surface morphology of the material. The material exhibited much higher discharge capacity of ~800 mAh/g after 65 cycles than that of graphite (372 mAh/g), the most commonly used anode material in industry. In addition, high charge rate testing is required to validate the material. Most work for fabrication of Mn_3O_4 is based on extremely low C-rate, and no work is carried out so far for ultra-fast charge and discharge.

Bibliography

1. Selin, Cynthia, Expectation and Emergence of Nanotechnology. Science, Techn ology & Human value. 2007, **32**(2), 196-220

2. Lee, Y. J. *et al*. Fabricating genetically engineered high-power lithium-ion batter ies using multiple virus genes. *Science* **324**, 1051–1055 (2009).

3. Nam. K. T et. al. Virus-Enabled Synthesis and Assembly of Nanowires for Lit hium Ion Battery Electrodes. *Science*, **312**, 885 (2006)

4. Lee, B.Y. *et al*. Virus-based piezoelectric energy generation. *Nature nanotechn ology*. **7**, 351-356 (2012).

5. Nuraje, N. *et al*. Biotemplated Synthesis of Perovskite Nanomaterials for solar Energy Conversion. Adv. Mater. **24**, 2885-2889 (2012)

6. Yi, H.; Ghosh, D.; Ham, M.H.; Qi, J.; Barone, P. W.; Strano, M.S; Belcer, A. M. M13 Phage-Functionalized Single-Walled Carbon Nanotubes As Nanoprobes for Second Near-Infrared Window Fluorescence Imaging of Trageted Tumors. *Nano Lett*. **12,** 1176-1183 (2012)

7. Mao, C *et. al.* Virus-Based Toolkit for the Directed Synthesis of Magnetic an d Semiconducting Nanowires. Science. **303**, 213-215 (2004).

8. Nam, K. T *et al*. Stamped microbattery electrodes based on self-assembled M1 3 viruses. PNAS. **105**, 17227-17231 (2008).

9. Mao. J.Y. *et al*. Genetically Engineered Phage Fibers and Coatings for Antiba cterial Applications. Adv. Funct. Mater. **20**, 209-214 (2010)

10. Crabtree, G.W and Lewis, N.S. Solar energy conversion. Physics Today , 37-48 (2007).

11. Gratzel, M. Solar Energy Conversion by Dye-sensitized Photovoltaic Cells. In

organic chemistry, **44**(20), 6841 (2005)

12. Picciotto. R *et al*. Four-terminal resistance of a ballistic quantum wire. Nature **411**, 51-54 (2001)

13. Wang, Y. *et al.* Catalytic growth and photoluminescence properties of semicon ductor single-crystal ZnS nanowire. Chemical Physics Lett. **357**(4), 314-318 (2 002).

14. Huang, Y. *et al.* Logic Gates and Computation from Assembled Nanowire Bui lding Blocks. Science **294**, 1313-1317 (2001).

15. Morales, A.M, *et al*. A laser Ablation Method for the synthesis of Crystalline Semiconductor Nanowires. Science **279**, 208 (1998).

16. Manna, L. *et al*. Synthesis of Soluble and Processable Rod-, Arrow-, Teardrop -, and Tetrapod-shaped CdSe Nanocrystals. J. Am. Chem. Soc. **122**, 12700-127 06 (2000).

17. Xia, Y. *et al*. One-Dimensional Nanostructures: Synthesis, Characterization and Applications. Advanced Materials 15 (5), 353-389 (2003).

18. Popov, V.N. Carbon nanotubes: properties and application. Materail science an d Engineering: R: Reports **43**(3), 61-102 (2004).

19. Melaiye, A. *et al*. Silver(I)-Imidazole Cyclophane gem-Diol Complexes Encaps ulated by Electrospun Tecophilic Nanofibers: Formation of Nanosilver Particles and Antimicrobial Activity. J. Am. Chem. Soc. **127**(7) 2285-2291 (2005).

20. Son, W. K. *et al.* Preparation of Antimicrobial Ultrafine Cellulose Acetate Fib ers with Silver Nanoparticles. Macromol. Rapid Commun. **25**, 1632-1637 (200 4)

21. Tarascon, J.M. and Armand, M. Building batter battery. Nature **451**, 652-657

(2008).

22. Cho, Y. K. *et al.* Self-assembling colloida-scale devices: Selecting and using s hort-ranged surface forces between conductive solids. Adv Funct Mater. **17,** 37 9-389 (2007).

23. Sidhu. S.S. *et al.* Engineering M13 for phage display. Biomolecular Engineerin g **18,** 57-63 (2001).

24. Cao. B. et al. Transmission Electron Microscopy as a Tool to Image Bioinorg anic Nanohybrids: The Case of Phage-Gold Nanocomposites. Microscopy Resea rch and Technique 74, 627-635 (2011).

25. Dong, D. *et al.* A simple and rapid method to isolate purer M13 phage by is oelectric precipitation. Appl. Microbiol. Biotechnol. **97**, 8023-8029 (2013)

26. Han, Y.F. *et al.* Observation of the Reversible Phase-Transformation of alpha Mn2O3 Nanocrystals during the Catalytic Combustion of Methane by in Situ Raman Spectroscopy. J. Phys. Chem. C **111** (7), 2830-2833 (2007)

27. Deng, Y. et al. Porous Mn2O3 microsphere as a superior anode material for l ithium ion batteries. RSC Adv. 2, 4645-4647 (2012).

28. Chen, K. Microwave-Hydrothermal Crystallization of Polymorphic MnO2 for E lectrochemcal Energy Storage. J. Phys. Chem. C. **117**, 10770-10779 (2013)

29. Scrosati, B. Recent advances in lithium ion battery materails. Electrochimica A cta **45**, 2461-2466 (2000).

30. Wakihara, M. Recent developments in lithium ion batteries. Materials Science and Engineering **33**, 109-134 (2001)

31. Guo, C.X. *et al.* A Hierarchically Nanostructured Composite of MnO2/ Conjug ated Polymer/Graphene for High-Performance Lithium Ion Batteries. Adv. Ener

gy Mater. **1**, 736-741 (2011).

32. Reddy, A.L.M *et al.* Coaxial MnO2/Carbon nanotube Array Electrodes for Hig h-Performance Lithium Batteries. Nano Lett. **9**(3), 1002-1006 (2009).

33. Debart, A. *et al.* Alpha MnO2 Nanowires: A Catalyst for the O2 Electrode Li thium Batteries. Angew. Chem. 120, 4597-4600 (2008).

34. Girishkumar. G. *et al.* Lithium-Air Battery: Promise and challenges. J. Phys. C hem. Lett. **1**, 2193-2203 (2010)

35. Lee, Y.J. *et al.* Fabricating Genetically Engineerred High-Power Lithium-Ion B attereis Using Multiple Virus Genes. Science **34**, 1051-1055 (2009).

36. Gao, J. **et al.** Spongelike Nanosized Mn3O4 as a High-Capacity Anode materi al for Rechargeable Lithium Batteries. Chem. Mater. *23*, 3223-3227 (2011)

37. Wang, J. *et al.* Mn3O4-Graphene Hybrid as a High-Capacity Anode Material f or Lithium Ion Batteries. J. Am. Chem. Soc. **132**, 13978-13980 (2010).

38. Pesero, D. Co-doped Mn3O4: a possible anode material for lithium batteries. J ournal of power sources **141**, 156-158 (2005).

39. Fang, T. The microstructural evolution of Mn3O4 hausmannite during autoxida tion. Key Engineering Matreials **280**, 693-698 (2004)

40. Fligiel, S.E. *et al.* Protein degradation following treatment with hydrogen peroxide. A m.J Pathol. **115**(3), 418-425 (1984).